BOWDENS
SILVER

Final Void Uncertainty Analysis Report

State Significant Development No. 5765

October 2022

Compiled by: **R.W. CORKERY & CO. PTY. LIMITED**

Bowdens Silver Project

Final Void Uncertainty Analysis Report

State Significant Development No. 5765

Prepared for:

Bowdens Silver Pty Limited
ABN: 37 009 250 051

Sydney Office
Level 28, 88 Phillip Street
SYDNEY NSW 2000

Telephone: (02) 8316 3997
Facsimile: (02) 8316 3999
Email: information@bowdenssilver.com.au

Operations Office
68 Maloneys Road
LUE NSW 2850
P.O. Box 1115
MUDGEE NSW 2850

Telephone: (02) 6373 6420

A Silver Mines Limited company

Compiled by:

R.W. Corkery & Co. Pty. Limited
Geological & Environmental Consultants
ABN: 31 002 033 712

Telephone: (02) 9985 8511
Email: admin@rwcorkery.com

Prepared in conjunction with:

HydroAlgorithmics Pty Ltd
Email: info@hydroalgorithmics.com

WRM Water and Environment
Telephone: (07) 3225 0200
Email: wrm@wrmwater.com.au

Jacobs Group (Australia) Pty Limited
Telephone: (02) 9928 2100
Email: sydney.reception@jacobs.com

Ref No. 429/42

October 2022

CONTENTS

Page

1 INTRODUCTION 1
1.1 SCOPE 1
1.2 APPROACH 1
1.3 SUMMARY OF OUTCOMES 3
1.4 MANAGEMENT OF INVESTIGATIONS 4

2 GROUNDWATER MODEL UNCERTAINTY ANALYSIS 5
2.1 METHODOLOGY 5
2.2 RESULTS 10

3 FINAL VOID WATER BALANCE MODEL UNCERTAINTY ANALYSIS 12
3.1 METHODOLOGY 12
3.2 FINAL VOID WATER BALANCE RESULTS 16

4 TESTING FINAL VOID BEHAVIOUR 20
4.1 METHODOLOGY 20
4.2 PARTICLE TRACKING OUTCOMES 22

5 REASONABLE MITIGATION MEASURES 25
5.1 CONSTRUCTED WETLANDS (INFILTRATION BASINS) 25
5.2 FINAL VOID GEOMETRY 25
5.3 GROUT INJECTION 26

6 UNCERTAINTY ANALYSIS MODELLING VS EIS GROUNDWATER MODELLING 27

7 DISCUSSION 29

8 REFERENCES 31

APPENDIX 1 CONVERGENCE OF GROUNDWATER MODEL UNCERTAINTY ANALYSIS 34
A1.1 CONVERGENCE 35

APPENDIX 2 DERIVATION OF PIT LAKE EVAPORATION FACTORS 39
A2.1 TOP-OF-PIT LAKE FACTOR 40
A2.2 SHADING 40
A2.3 WIND SHELTERING 43

FIGURES

Figure 1 Layout of Pilot Points Relative to the Model Grid 7
Figure 2 Inflow to the pit by stage 11
Figure 3 Stage-inflow relationships for Final Void Monte Carlo Model and WRM 2022 Model 13
Figure 4 Modelled annual pit lake evaporation factor at all elevations 15

CONTENTS

Page

Figure 5	CDF for pit lake evaporation factor at 574mAHD compared to previous WRM modelling	15
Figure 6	Results of Monte Carlo analysis – final void water level	16
Figure 7	Probability of peak water level exceedance	17
Figure 8	Modelled Pit Evaporation factor for Realisation 3,158 (red line) compared to PDF	18
Figure 9	Modelled Pit Runoff C_{avg} for Realisation 3,158 (red line) compared to PDF	18
Figure 10	Modelled Rehab Runoff C_{avg} for Realisation 3,158 (red) compared to PDF	19
Figure 11	Proposed constructed wetlands – augmented eastern wetland	22
Figure 12	95th Percentile Final Void Pit Lake Water Levels – Unmitigated Particle Tracking	23
Figure 13	95th Percentile Final Void Pit Lake Water Levels – Mitigated Particle Tracking	24
Figure 14	Modelled Infiltration Basin Locations and Particle Seed Points	24
Figure 15	Relationship Between Maximum Pit Lake Water Level and Pit Lake Evaporative Surface Area (from Realisation 3,158)	26
Figure 16	Change in Inflow Percentiles with Number of Model Runs at a Pit Lake Stage of 560mAHD	36
Figure 17	99.7% Confidence Intervals for Inflow Percentiles at a Pit Lake Stage of 560mAHD	36
Figure 18	Change in Inflow Percentiles with Number of Model Runs at a Pit Lake Stage of 579mAHD	37
Figure 19	99.7% Confidence Intervals for Inflow Percentiles at a Pit Lake Stage of 579mAHD	37
Figure 20	Change in Inflow Percentiles with Number of Model Runs at a Pit Lake Stage of 590mAHD	38
Figure 21	99.7% Confidence Intervals for Inflow Percentiles at a Pit Lake Stage of 590mAHD	38
Figure 22	Top-of-pit PDF (black line) and previously adopted values	40
Figure 23	Monthly Variation in Shortwave Radiation at Various Water Elevations	41
Figure 24	Shading Factors for Adjusting Morton's Shallow Lake Evaporation	42
Figure 25	Shading Factor used to Produce Pit Factor over the Range of Elevations	42
Figure 26	Windspeed multiplier compared to McJannet et al 2016	44
Figure 27	Sheltering factor over full range of elevations	44

TABLES

Table 1	Hydraulic Conductivity Distributions	8
Table 2	Storage Distributions	8
Table 3	Recharge Factor Distributions	9
Table 4	PDFs for AWBM runoff parameters	14
Table 5	Average annual water balance – Realisation 3,158 vs Previous Analysis	17
Table 6	Updated Hydraulic Parameters – Model Run 288	20
Table 7	Parameters Defining the Proposed PDF for the Top-of-pit Lake Factor	40

1 Introduction

1.1 Scope

This Uncertainty Analysis has been compiled to provide a response to a recommendation made in the *Bowdens Silver Project Groundwater Assessment Review* prepared by HydroGeoLogic Pty Ltd. The review was provided to Bowdens Silver Pty Limited (Bowdens Silver) on 23 May 2022. Specifically, the assessment presented in this document responds to the following comment contained in the HydroGeoLogic review.

> *Based on the evidence presented in the groundwater assessment reports of the non-trivial potential for final void lake throughflow conditions to develop in the post-mining period, this review recommends that a quantitative uncertainty analysis be conducted consistent with recent guidance (Middlemis et al. 2018, 2019). If the findings confirm the (non-trivial) potential, then detailed geochemical analysis of the final void lake water quality may be required to define the source concentrations of potential contaminants, and transport and fate assessments may be required for the pathways to receptors, notably Hawkins Creek.*

Two meetings were convened by the Department of Planning and Environment (DPE) with HydroGeoLogic, Bowdens Silver and the authors of this document on 22 June 2022 and 30 August 2022 to discuss the approach to the Uncertainty Analysis.

In February 2022, WRM Water and Environment Pty Ltd (WRM) prepared an Updated Surface Water Assessment (WRM, 2022) supporting the Water Supply Amendment Report for the Bowdens Silver Project (the Project). The WRM (2022) report outlined sensitivity testing of the final void water balance model which identified that under a high groundwater inflow scenario, high pit lake water levels could potentially result. The upper bound water level predicted under this scenario was equal to the previously predicted water level at which the final void would cease being a groundwater sink and become a through flow system, with outflow from the final void pit lake potentially entering the groundwater setting. This outcome was at odds with the predictions of the EIS groundwater model presented in the *Updated Groundwater Assessment* prepared by Jacobs (2022), also prepared in support of the Project's Water Supply Amendment Report. Although the EIS groundwater model calibration was considered to reasonably match recorded parameters in the groundwater setting, it was agreed that an Uncertainty Analysis would be used to test the application of modelling parameters in the groundwater model and the final void water balance model.

1.2 Approach

This Uncertainty Analysis has involved a multi-disciplinary assessment of uncertainty pertaining to parameters applied in modelling of groundwater and surface water behaviour in the proposed final void for the Bowdens Silver Project (the Project). Uncertainty associated with hydraulic conductivity, recharge factors, specific storage and specific yield properties within the groundwater model was tested via stochastic modelling of randomly selected parameter sets for multiple model realisations to generate a probable range of groundwater inflow rates. Further uncertainty analysis of parameters for catchment runoff and pit lake evaporation was undertaken using the Monte Carlo modelling capabilities of the GoldSim final void water balance model.

In summary the approach taken to the Uncertainty Analysis involved the following key steps.

- Uncertainty analysis of groundwater modelling parameters by HydroAlgorithmics including:
  - linking the separate calibration, operations and recovery groundwater models;
  - undertaking the Latin Hypercube Sampling (LHS) method for simulation of the linked groundwater model using 500 separate realisations that randomly sample model properties and recharge factors from a range of values; and
  - using the range in inflow outcomes generated by the LHS realisations, produce a family of groundwater inflows versus lake levels for input to the GoldSim model. Of the 500 realisations, 449 were accepted, 2 were rejected due to non-convergence and 49 were rejected because they exceeded the calibration constraint.
- Groundwater inflow outcomes generated by HydroAlgorithmics was then applied to the GoldSim final void water balance model by WRM to permit a further Monte Carlo analysis, also using LHS, of the pit lake's evolution and behaviour.

  The WRM analysis utilised 5,388 model realisations. Each of 449 selected groundwater inflow versus lake level curves provided by HydroAlgorithmics was sampled 12 times, along with random samples from a range of:
  - top of pit factors applied to daily Morton's shallow lake evaporation estimates for the Mine Site obtained from SILO to estimate evaporation from a lake at the natural pit top ground level;
  - factors applied to the pit top lake evaporation to account for the influence of shading and wind sheltering when the lake is at lower levels, including the influence of seasonal variation; and
  - catchment runoff parameters.

  The Monte Carlo analysis undertaken by WRM was used to identify the exceedance probability of a specified final void peak pit lake water level and establish the behaviour of the final void in the groundwater setting.

Based on these results, Jacobs applied the 95th percentile final void peak lake water level (low probability outcome) to the EIS groundwater model. Particle tracking was applied to assess the potential seepage paths and rates from the final void. The groundwater model was run by Jacobs with no mitigation and then with mitigation of seepage applied.

1.3 Summary of Outcomes

The Uncertainty Analysis has identified that at higher pit lake levels, through flow conditions may develop in some sections of the void. Given that the final void lake would be present in perpetuity and that evapoconcentration of salts, acids and metals may occur over time, Bowdens Silver has committed that the final landform would incorporate passive controls that restrain or remove the occurrence of through flow.

Modelling of final void behaviour has served to demonstrate that, in the event that the final void is considered likely to develop to a through flow system:

- the groundwater gradient adjacent to the final void, in areas of potential outflow would be relatively low (between 0.0051 and 0.0161);
- the average groundwater gradient between final void and Hawkins Creek would be 0.02;
- following equilibrium, travel time to Hawkins Creek would be in the order of 100 to 200 years); and
- the potential risk of seepage impacting downgradient receptors can be readily managed and mitigated.

Measures that have been considered to mitigate seepage include the following.

- Constructing wetlands that artificially recharge the groundwater setting at key locations adjacent to the final void, thus locally reversing hydraulic gradients to prevent outflow from the final void.
- Amending final void geometry to increase the evaporative surface of the pit lake, thus depressing lake levels and reducing likelihood of through flow conditions developing.
- Applying grouting at select locations within the final void to provide a barrier to groundwater flow.

Modelling of the low probability 95th percentile final void water level outcome in the EIS groundwater model incorporating a constructed wetland as mitigation demonstrates that successful passive mitigation can be achieved and would therefore also be more readily achievable for more likely scenarios with lower void water levels. Further to this, assessment of the benefits from changing final void geometry also support its potential adoption as a passive mitigation measure. Finally, grouting is a well-known mitigation measure with numerous established practical applications.

Bowdens Silver maintains its position that geochemical analysis of the final void lake water quality is not required given that water is not likely to enter the groundwater setting, either as a result of the proposed design of the final void or through the inclusion of simple mitigation measures.

Bowdens Silver has also committed to the progressive review of the groundwater model developed for the Project to provide for model updates as mining progresses and more data is collected. This approach would provide the means for continuous improvement that ensures modelling assumptions are progressively tested and validated through physical results. This would then allow robust testing and assessment of all proposed closure strategy(ies) such that any measure (if required) could be adopted with confidence.

1.4 Management Of Investigations

This document has been prepared by a team managed by R.W. Corkery & Co. Pty Limited (RWC) and included the following authors.

- Mr Michael Batchelor (MEngSt., BE (Hons)) of WRM Water and Environment Pty Ltd.
- Dr Damian Merrick - (PhD, BCST (Hons)) of HydroAlgorithmics Pty Ltd.
- Dr Noel Merrick (PhD, MSc., BSc.) of HydroAlgorithmics Pty Ltd.
- Mr Paul Ryall (BSc. (Hydrology and Water Resources)) of RWC.
- Mr Greg Sheppard (MSc (Eng. Geology), BSc(Geology)) of Jacobs Pty Ltd.
- Mr Nicholas Warren (MEnv.Sc., MBus., BSc.) of RWC.

2 Groundwater Model Uncertainty Analysis

2.1 Methodology

2.1.1 Introduction

The following presents the methodology applied by HydroAlgorithmics in assessing the uncertainty in groundwater inflows to the final void after mining has finished. The methods applied by HydroAlgorithmics are consistent with the *Guidance for groundwater modelling within a risk management framework. Report for Independent Expert Scientific Committee (IESC) on Coal Seam Gas and Large Coal Mining Development* (Middlemiss and Peeters, 2018).

The Groundwater Model Uncertainty Analysis addresses parameter uncertainty by stochastic modelling using the Latin Hypercube Sampling (LHS) method: generating numerous alternative parameterisations of the deterministic flow model (realisations), executing the model independently for each, and then aggregating the results for statistical analysis. Whilst LHS is similar to the classical Monte Carlo method, it utilises a stratified sampling technique which typically provides faster convergence.

A traditional drawback to the Monte Carlo and LHS methods is that their successful application often necessitates hundreds or thousands of model runs, each of which may take several hours of run time on a modern computer. More complex variants of Monte Carlo exist which aim to explore the parameter space more efficiently than the basic Monte Carlo approach, such as Null Space Monte Carlo (NSMC) (Doherty, 2015) and Markov Chain Monte Carlo (MCMC) approaches (e.g. Vrugt et al., 2009).

However, recent offerings in the field of cloud computing have greatly increased the availability and accessibility of computing resources, allowing hundreds of model runs to be evaluated simultaneously. Owing to this, HydroAlgorithmics elected to use the LHS approach, which places no reliance on a linearisation of the model, allows for each individual model run to be kept relatively simple and with predictable run time (no additional calibration steps), and is free from the problem of autocorrelated samples that may occur with MCMC approaches.

AlgoCompute (HydroAlgorithmics, 2019 and Merrick, 2017) was used as the platform for executing the model runs in parallel; up to 272 realisations were evaluated simultaneously, being allocated over 91 virtual machines in the cloud. The model-independent uncertainty quantification software HGSUQ (Miller et al., 2018) was used to generate the LHS parameter realisations and orchestrate the model runs within the AlgoCompute environment.

2.1.2 Parameters

Uncertainty was assessed on hydraulic conductivity, recharge factors, specific storage and specific yield properties within the groundwater model[1]. Pilot points were used for conductivity and storage properties to allow them to vary spatially throughout the model. The AlgoMesh software (Merrick and Merrick, 2015) was used to distribute 120 pilot points over the model domain, with separation between adjacent points varying between approximately 220m (within the Mine Site) and 10km (along the outer model extents). The resulting layout of pilot points is shown in **Figure 1**. The densest grouping in the immediate vicinity of the Mine Site comprises 29 points in the vicinity of the main open cut pit that would form the final void.

The complete set of 120 pilot points was duplicated for each material property zone in the model within layers 1 to 6, and then trimmed for each zone to include only those points inside and immediately adjacent to the borders of the zone. For each zone, statistical distributions were assigned at each pilot point for horizontal hydraulic conductivity (Kx), vertical anisotropy (Kx/Kz), specific storage (Ss) and specific yield (Sy) parameters based on the calibrated model values for that zone, from which randomly sampled values were generated for each evaluated model realisation. The parameter values at the pilot points were subsequently interpolated to model cells by kriging. Properties in layers 7 and 8 (basement) were left at their calibrated constant values.

In addition to conductivity and storage parameters, recharge factors for the closest recharge zones to the Mine Site (recharge zones 1-4) were assigned distributions conservatively across the entire respective zone. No pilot point variation was used for the recharge factor parameters.

In total across all zones and parameter types, 4,348 individual parameters were included in the uncertainty analysis. As there are no guidelines on selection of prior distributions, the professional judgement of HydroAlgorithmics, based on substantial experience, has been relied upon to assign truncated log-normal (Kx, Ss, Sy), log-uniform (Kx/Kz vertical anisotropy ratio) and uniform (recharge factor) distributions. As Kx/Kz is eventually converted to Kz, the Kz property implicitly also has a log-normal distribution, as is observed to occur in nature. As recharge factor is poorly defined by typical groundwater datasets, a uniform distribution is more conservative than a normal distribution over a wider range of values.

A log standard deviation of 0.5 was applied for the prior distributions of hydraulic conductivity (Kx)and specific storage (Ss) parameters, such that randomly sampled values should lie within one order of magnitude (two standard deviations) either side of the calibrated parameter values. For specific yield (Sy), a lower standard deviation of 0.25 was used to ensure a physically reasonable range of values (half an order of magnitude either side of the calibrated values), and values were capped at a maximum of 0.4 (based on professional judgement of maximum physically possible porosity). Vertical anisotropy (Kx/Kz) parameters were assigned log-uniform distributions with an upper bound of ten times the calibrated value, and a lower bound of one tenth the calibrated value, capped to a minimum of 1 to ensure Kz ≤ Kx.

[1] The calibration, operations and recovery groundwater models are those documented in Jacobs (2022); the recovery model is termed Variant A (High-K lake with K=1000m/day and Sy=1; with no direct rainfall on the void or evaporation from the pit lake). The models were linked sequentially by starting each model using the output heads from the end of the preceding model.

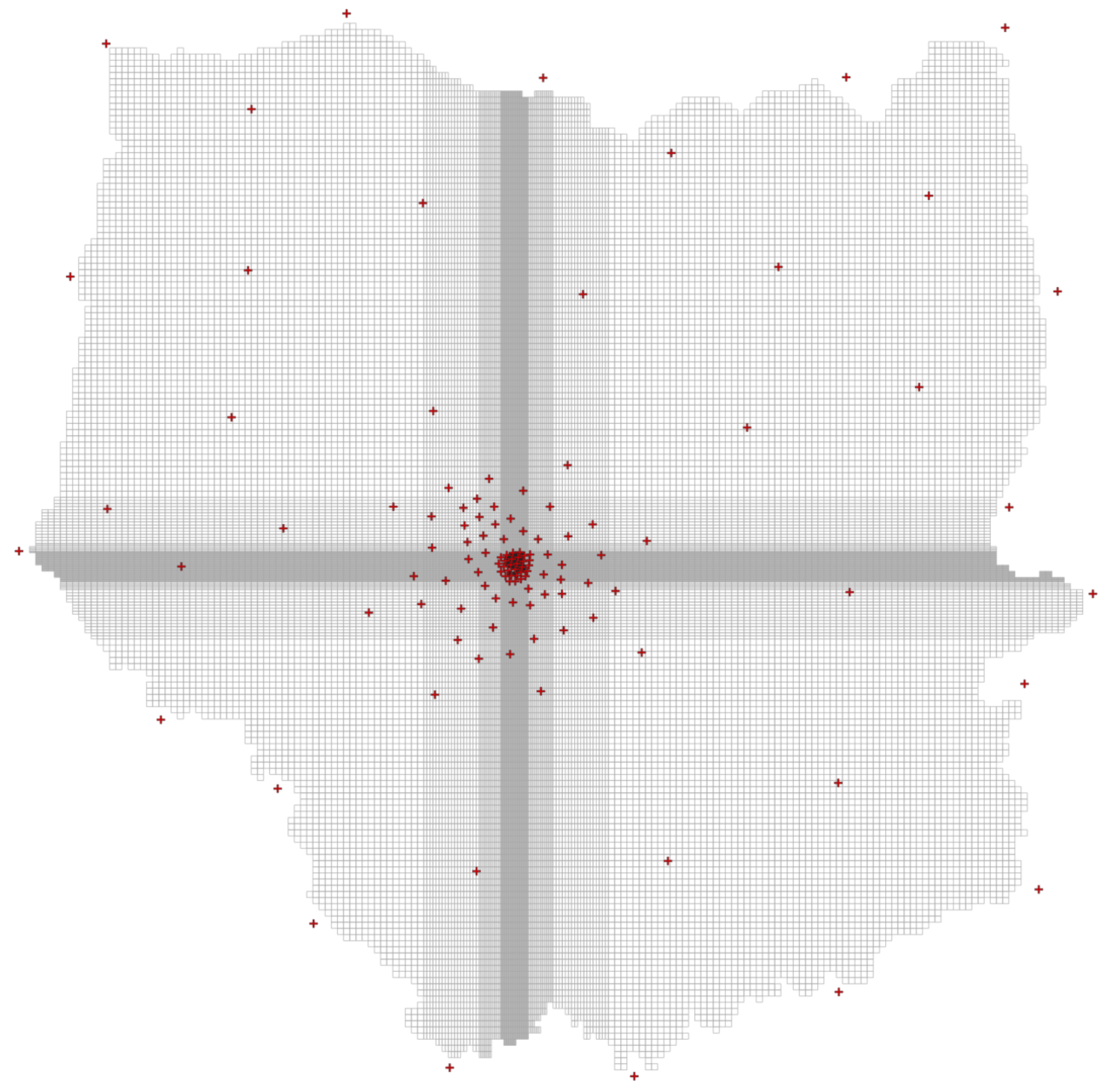

Figure 1
Layout of Pilot Points Relative to the Model Grid

The resulting hydraulic conductivity, storage and recharge factor distributions are listed in **Table 1**, **Table 2** and **Table 3** respectively. The recharge factor distributions are designed to be symmetrical around the calibrated values, with the maximum value for Zone 1 set at 1.5 times the calibrated value to constrain the maximum (18%) at a value regarded as a physical limit of foothills recharge (based on the professional judgement of HydroAlgorithmics). The same 1.5 multiplier is applied to the other recharge zones. The minimum values are determined by subtraction to maintain symmetry.

Table 1
Hydraulic Conductivity Distributions

Layer	K Zone	Description	Kx (truncated log-normal, log stdev 0.5)			Kx/Kz (log-uniform)	
			Mean	Min	Max	Min	Max
1	11	Alluvium (sandy silt)	2.06	2.1×10^{-1}	20.57	1	19.31
	12	Regolith (clayey silt with vegetation)	9.8×10^{-2}	9.8×10^{-3}	9.8×10^{-1}	1	11.59
	13	Weathered rock	1.0×10^{-1}	1.0×10^{-2}	1.00	1	50
2	21	Alluvium (silty sand)	3.00	3.0×10^{-1}	30.00	1	50
	22	Extremely weathered rock (silty clay)	5.0×10^{-2}	5.0×10^{-3}	5.0×10^{-1}	1	50
	23	Weathered rock	2.5×10^{-1}	2.5×10^{-2}	2.50	1	50
3	31	Partially weathered rock (with stiff clay)	8.9×10^{-1}	8.9×10^{-2}	8.93	9.93	992.74
	32	Partially weathered rock	5.7×10^{-1}	5.7×10^{-2}	5.68	1.02	101.51
	33	Weathered rock	8.7×10^{-1}	8.7×10^{-2}	8.74	1	87.91
4	41	Ordovician basement	3.0×10^{-3}	3.0×10^{-4}	3.0×10^{-2}	1	100
	42	Sydney basin	3.0×10^{-3}	3.0×10^{-4}	3.0×10^{-2}	1	100
	45	Rylstone volcanics / Coomber formation	6.0×10^{-2}	6.0×10^{-3}	6.0×10^{-1}	1	50
	46	Rylstone volcanics	1.0×10^{-1}	1.0×10^{-2}	1.00	1	50
5	51	Rylstone volcanics / Ordovician basement	2.6×10^{-3}	2.6×10^{-4}	2.6×10^{-2}	1	63.99
	52	Sydney basin	2.1×10^{-3}	2.1×10^{-4}	2.1×10^{-2}	1	53.65
	53	Rylstone volcanics / Coomber formation	2.0×10^{-2}	2.0×10^{-3}	2.0×10^{-1}	1	100
	55	Rylstone volcanics / Coomber formation	2.0×10^{-1}	2.0×10^{-2}	2.00	1	100
6	61	Ordovician basement	2.3×10^{-4}	2.3×10^{-5}	2.3×10^{-3}	1	57.73
	63	Rylstone volcanics / Coomber formation	1.0×10^{-2}	1.0×10^{-3}	1.0×10^{-1}	1	50

Table 2
Storage Distributions

Layer	S Zone	Ss (truncated log-normal, log stdev 0.5)			Sy (truncated log-normal, log stdev 0.25)		
		Mean	Min	Max	Mean	Min	Max
1	11	9.0×10^{-4}	9.0×10^{-5}	9.0×10^{-3}	0.11	0.035	0.35
	12	9.0×10^{-4}	9.0×10^{-5}	9.0×10^{-3}	0.09	0.028	0.28
	13	5.0×10^{-5}	5.0×10^{-6}	5.0×10^{-4}	0.02	0.0063	0.063
2	21	7.0×10^{-4}	7.0×10^{-5}	7.0×10^{-3}	0.30	0.095	0.40
	22	7.0×10^{-4}	7.0×10^{-5}	7.0×10^{-3}	0.04	0.013	0.13
	23	5.0×10^{-5}	5.0×10^{-6}	5.0×10^{-4}	0.02	0.0063	0.063
3	31	5.0×10^{-4}	5.0×10^{-5}	5.0×10^{-3}	0.09	0.028	0.28
	32	5.0×10^{-4}	5.0×10^{-5}	5.0×10^{-3}	0.09	0.028	0.28
	33	5.0×10^{-5}	5.0×10^{-6}	5.0×10^{-4}	0.02	0.0063	0.063
4	41	2.0×10^{-5}	2.0×10^{-6}	2.0×10^{-4}	0.01	0.0032	0.032
	42	4.0×10^{-5}	4.0×10^{-6}	4.0×10^{-4}	0.02	0.0063	0.063
	(Rest of L4)	5.0×10^{-5}	5.0×10^{-6}	5.0×10^{-4}	0.01	0.0032	0.032
5	51	2.0×10^{-5}	2.0×10^{-6}	2.0×10^{-4}	0.01	0.0032	0.032
	52	2.0×10^{-5}	2.0×10^{-6}	2.0×10^{-4}	0.01	0.0032	0.032
	(Rest of L5)	2.0×10^{-5}	2.0×10^{-6}	2.0×10^{-4}	0.01	0.0032	0.032
6	*(All)*	2.0×10^{-5}	2.0×10^{-6}	2.0×10^{-4}	0.01	0.0032	0.032

Table 3
Recharge Factor Distributions

Recharge Zone	Description	Recharge Factor *(uniform)*		
		Calibrated	Min	Max
1	Foothills	0.12	0.06	0.18
2	Hilltops	0.02	0.01	0.03
3	Hilltops	0.04	0.02	0.06
4	Floodplain	0.03	0.015	0.045

2.1.3 Run Procedure

For each LHS realisation, the following procedure was executed on a virtual machine in the cloud, initiated by a HGSUQ worker process:

1. Interpolate pilot point parameter values to model cells using PLPROC (Doherty, 2016) and produce corresponding data files for inclusion in the model LPF package inputs.
2. Multiply recharge factors by rainfall to generate model RCH package inputs.
3. Run calibration period model (including an initial steady-state period to establish initial heads).
4. Run transient prediction (operations period) model.
5. Run transient recovery model.
6. Process model result files to compute calibration statistics and predictive outputs (stage-inflow curves) and return these to the HGSUQ "master" process for amalgamation with other run results.

2.1.4 Modelling Outcome Convergence

When conducting stochastic modelling, it is important to ensure that enough realisations are evaluated such that the results reported are accurate – that is, that the stochastic process has *converged* to within an acceptable probabilistic margin of error. This is particularly important for the stage-inflow output curves: due to the varied input properties, not every run is guaranteed to exhibit the entire range of pit lake stages. That is, for each pit lake stage, only a subset of the calibration-constrained runs reported an inflow at that stage.

To gain confidence that the reported results were sufficiently close to their correct values, 99.7% confidence intervals were computed for the 10%, 33%, 50%, 67% and 90% probabilities of exceedance of selected aggregate metrics.

Confidence interval bounds for the $(100 \times p)^{\text{th}}$ percentile may be approximated by the formula $p \pm \sqrt{p(1-p)c^2/n}$, where c is the desired confidence in standard deviations of the normal distribution – $c = 3$ for 99.7% confidence – and n is the number of runs (see e.g. Mood et al., 1974 for derivations of confidence interval bounds). For example, it may be said with 99.7% confidence after 449 successful runs that the true 90th percentile value lies between the 85.7th and 94.3rd percentile estimates $(= 100 \times \left(0.9 \pm \sqrt{0.9 \times 0.1 \times 9/449}\right))$. Details of the convergence achieved for the random sampling process for groundwater inflows are presented in **Appendix 1**.

2.1.5 Assumptions

The following assumptions should be noted in assessing the information presented in the Uncertainty Analysis of the groundwater model.

- The stochastic modelling performed was limited to the parameters described in Section 2.1.2. Uncertainty was not assessed on any other aspect of the groundwater model.
- Spatial variability was assessed only to the resolution of the pilot point set, and within the limits of the delineated property zones.
- Assessment of uncertainty in recharge was restricted to a single recharge factor parameter for each of the four recharge zones closest to the Mine Site.
- Each calibrated realisation was assumed to be equally likely in the analysis of the model outputs, i.e. apart from rejecting particularly poorly-calibrated runs, no weighting was applied to distinguish models based on how well they fit the observed data.

2.2 Results

In total, 500 realisations were evaluated as part of the LHS process. A calibration constraint on the scaled root-mean square (SRMS) error within 4km of the Mine Site was applied such that models were rejected if they exhibited a transient SRMS error at or above the 90th percentile of all realisations[2] (7.09%). Of the 500 realisations, 449 were accepted, 2 were rejected due to non-convergence and 49 were rejected because they exceeded the calibration constraint.

The stage-inflow curve was taken from each accepted realisation and combined into a family of curves that was subsequently used as input to the GoldSim modelling process. The distribution of inflows from these curves can be seen as 10%, 33%, 50%, 67% and 90% probabilities of exceedance in **Figure 2**.

[2] The 90th percentile was used as a calibration constraint instead of the typical 10% SRMS suggested by Australian Groundwater Modelling Guidelines (Barnett et al, 2012) because all realisations exhibited well under 10% SRMS (even when limited locally to the Mine Site). This criterion was put in place to ensure that the analysis was still informed by the fit to historical data.

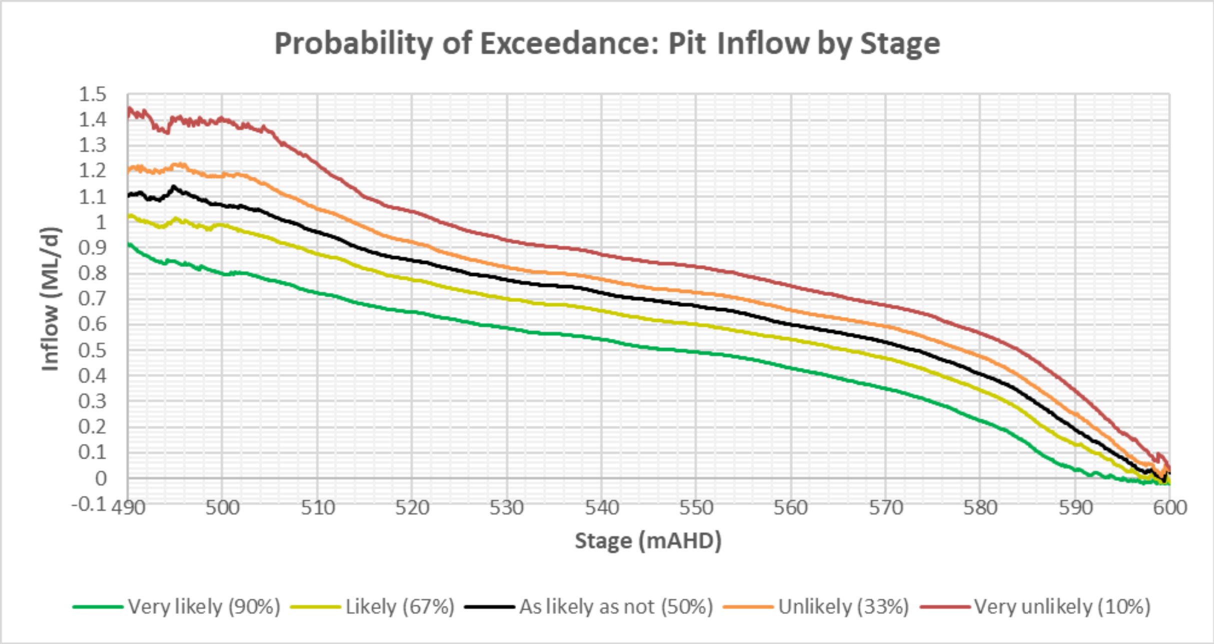

Figure 2
Inflow to the pit by stage

3 Final Void Water Balance Model Uncertainty Analysis

3.1 Methodology

3.1.1 Introduction

The methodology applied by WRM to undertake the Final Void Water Balance Model Uncertainty Analysis is presented in the following subsections. WRM assessed uncertainty in parameter assumptions relating to the likely long-term final void water level to better understand the likelihood of encountering groundwater through flow conditions.

WRM used the Monte Carlo modelling capabilities of the GoldSim software to probabilistically represent parameter uncertainty using LHS. The input parameters modelled stochastically by the GoldSim software included:

- groundwater inflow;
- catchment runoff; and
- pit lake evaporation.

For the previous (WRM, 2022) final void water balance studies, WRM adopted prudently conservative estimates of these parameters coupled with a stage-inflow curve provided by Jacobs.

3.1.2 Model Modifications

The schematisation of the GoldSim model was largely unchanged from that used in WRM's 2022 assessment. However, the runoff modelling approach was refined slightly, and the climate data was updated, as briefly outlined below.

Runoff Model Changes

The catchment runoff inflow component was refined to better differentiate the runoff response of pit walls and hard rock faces compared to rehabilitated benches within the pit catchment. The adopted catchment types were as follows.

- Hard rock pit surfaces: 41.3ha
- Rehabilitated benches: 8.8ha

Climate Data Sources

For consistency with the EIS, the GoldSim model adopted a wrapped historical climate sequence. However, the historical climate data was contemporised using the latest available SILO dataset that reflects revisions based on updates to Bureau of Meteorology data inputs and changes to

SILO interpolation techniques. The approach to climate change effects was the same used in the WRM (2022) modelling whereby the most likely climate scenario (HI.H) under the RCP4.5 2070 AR5 pathway was adopted.

3.1.3 Parameters

When running a probabilistic simulation or Monte Carlo model, GoldSim repeats the historical simulation many times (more than 5,000), with each simulation or "realisation" representing a possible "future" for the system. For each realisation, the key input parameters are resampled from pre-defined probability distribution functions (PDFs) at the start of each simulation. Details of the adopted PDF are provided in the following sections.

Groundwater Inflow

As noted in Section 2.2, HydroAlgorithmics generated 449 stage-inflow curves from realisations that met SRMS criteria. These were then applied to the existing GoldSim final void water balance model. This allowed for uncertainty in the stage-inflow relationship to be incorporated into the final void water balance model whereby each GoldSim model realisation sampled a stage-inflow curve for use in the entire realisation to establish the evolution of pit lake levels over time.

The GoldSim model was configured to sample each of the 449 stage-inflow curves the same number of times (12) across the full suite of 5,388 realisations. **Figure 3** compares the percentile bands of the HydroAlgorithmics stage-inflow curves to that used in WRM (2022). This figure shows that groundwater inflows at equilibrium water levels are generally elevated when compared with those used for WRM's 2022 modelling (refer blue line on **Figure 3**). For example, at an elevation of 575mAHD, the median inflow from HydroAlgorithmics is 0.48ML/day, compared to the previously adopted 0.2ML/day.

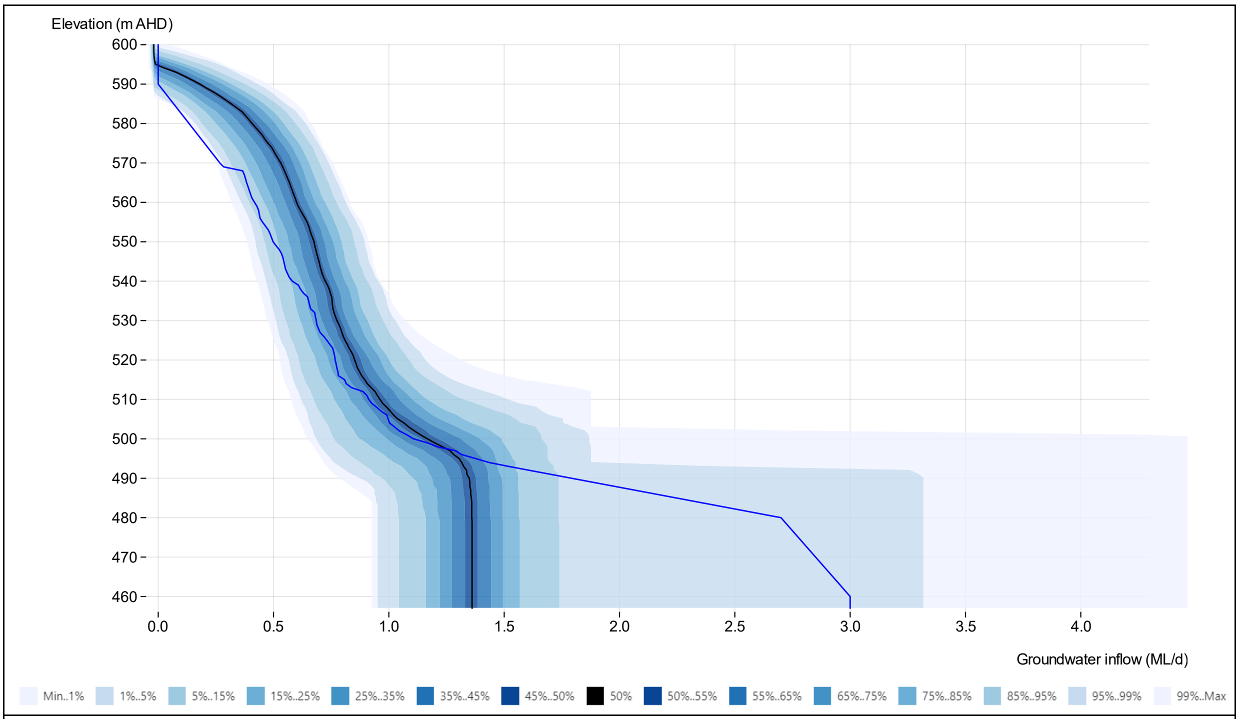

Figure 3
Stage-inflow relationships for Final Void Monte Carlo Model and WRM 2022 Model

Runoff Characteristics

Triangular PDF were applied to the USC parameter values of the Australian Water Balance Model (AWBM) in each modelled catchment. The PDF were configured so that sampled values from USC2 and USC3 were correlated with USC1.

The adopted triangular PDF parameters are summarised in **Table 4** below.

For the rehabilitated areas, the minimum USC values reflect those adopted for the high runoff scenario used in the site water balance model sensitivity analysis (refer Table 5.10 of WRM [2022]). However, the maximum USC values shown for rehabilitated areas in **Table 4** are slightly lower than those used for sensitivity testing of a low runoff scenario in the site water balance model respectively (refer Table 5.9 of WRM [2022]). This was done to provide additional conservatism in the form of higher runoff contributions to the pit lake, in lower runoff realisations. The most likely USC values are the same as those presented in Table 5.10 of WRM (2022) for natural/undisturbed catchments in the high runoff scenario.

Table 4
PDFs for AWBM runoff parameters

AWBM Parameters	Pit walls / Hard rock			Rehabilitation		
	Min (max runoff)	Most likely	Max (min runoff)	Min (Max runoff)	Most likely	Max (Min runoff)
USC1 (mm)	1.25	2.5	5	11	25	70
USC2 (mm)	2.5	5	10	60	95	170
USC3 (mm)	5.0	10	20	130	150	200
C_{Avg} (mm)	3.4	6.8	13.7	83.7	109	170
C_{Avg} (mm) WRM 2022			13.7	83.7	114	172
Similar WRM 2022 classification			Pit High	Rehab High	Natural High	Rehab Low

Pit Lake Evaporation Factors

Typical pan factors for lakes and dams are well understood through published research and WRM's calibrations to other site water balance models. However, the available data for deep void pit lakes is very limited, and the subject of ongoing research (e.g. McJannet, 2019). In WRM's previous (2022) assessment, evaporation factors were linearly interpolated with pit lake water level, between an adopted pit top factor (0.88 (base case) and 0.75 (sensitivity analysis) and 0.5 at the pit floor, to account for the effect of shading and sheltering.

For this analysis, an attempt was made to better reflect the uncertainty in evaporation estimates by accounting for the physical characteristics of the final void. The pit lake evaporation factor was therefore calculated by multiplying the sampled top-of-pit lake factor by:

- a shading factor derived from analysis of the effect of shading on solar radiation reaching the lake surface, similar to that adopted for the CSIRO evaporation model (McJannet, 2017); and
- a sheltering factor derived from a relationship between windspeed and depth below ground surface derived with reference to a small number of observations from research by CSIRO (McJannet, 2016).

The resultant pit lake evaporation factors, shown in **Figure 4**, exhibit increasing uncertainty with depth below ground level. Further details of the shading and sheltering factors used to derive this relationship are provided in **Appendix 2**.

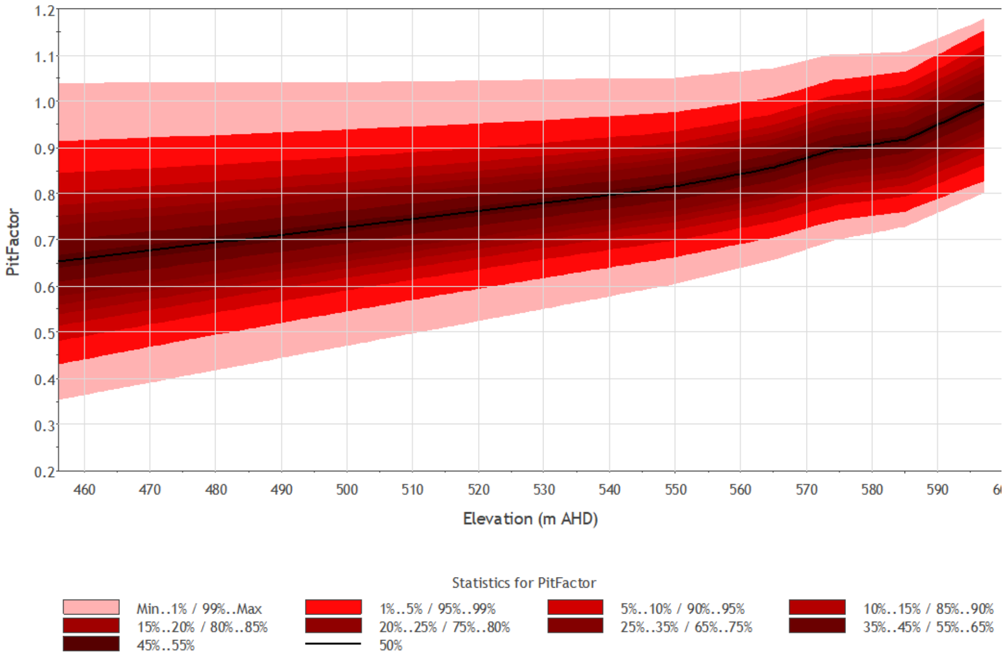

Figure 4
Modelled annual pit lake evaporation factor at all elevations

Figure 5 compares the resultant cumulative distribution function (CDF) of annual pit lake evaporation factor at 574mAHD (23m below the pit top elevation) to the previously adopted values.

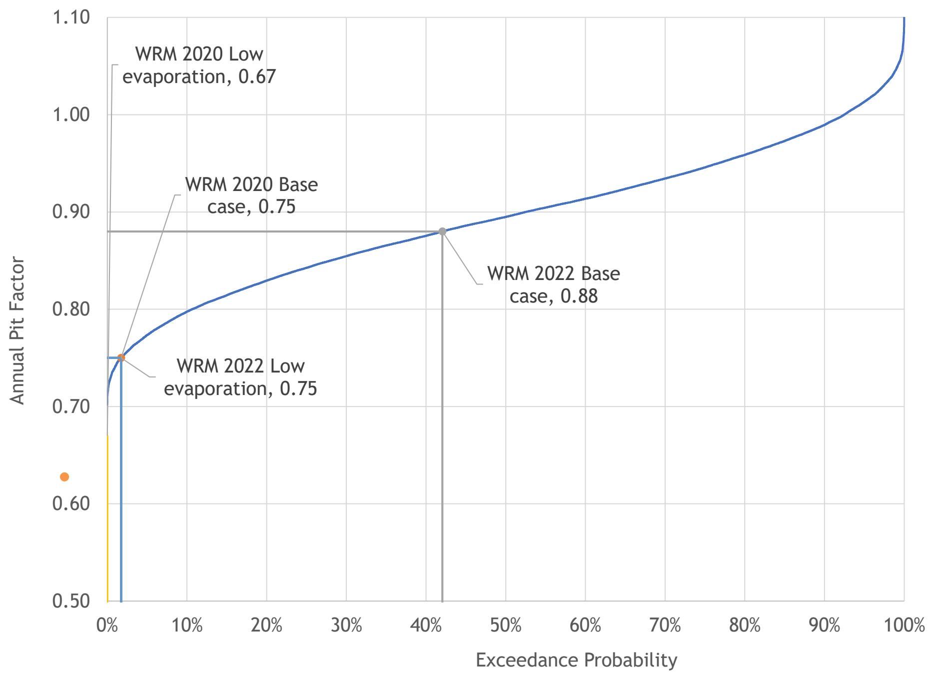

Figure 5
CDF for pit lake evaporation factor at 574mAHD compared to previous WRM modelling

3.2 Final Void Water Balance Results

The GoldSim model was run as a probabilistic simulation for 5,388 realisations, with each of the 449 stage-inflow curves being used 12 times. The results of the analysis are shown in **Figure 6**, which shows the modelled water level over the probabilistic simulation period in terms of percentile bands.

As shown on **Figure 6**, approximately 140 years after closure, the pit lake reaches dynamic equilibrium with the median percentile trace then varying between 574.2mAHD and 580.7mAHD throughout the remainder of the simulation period.

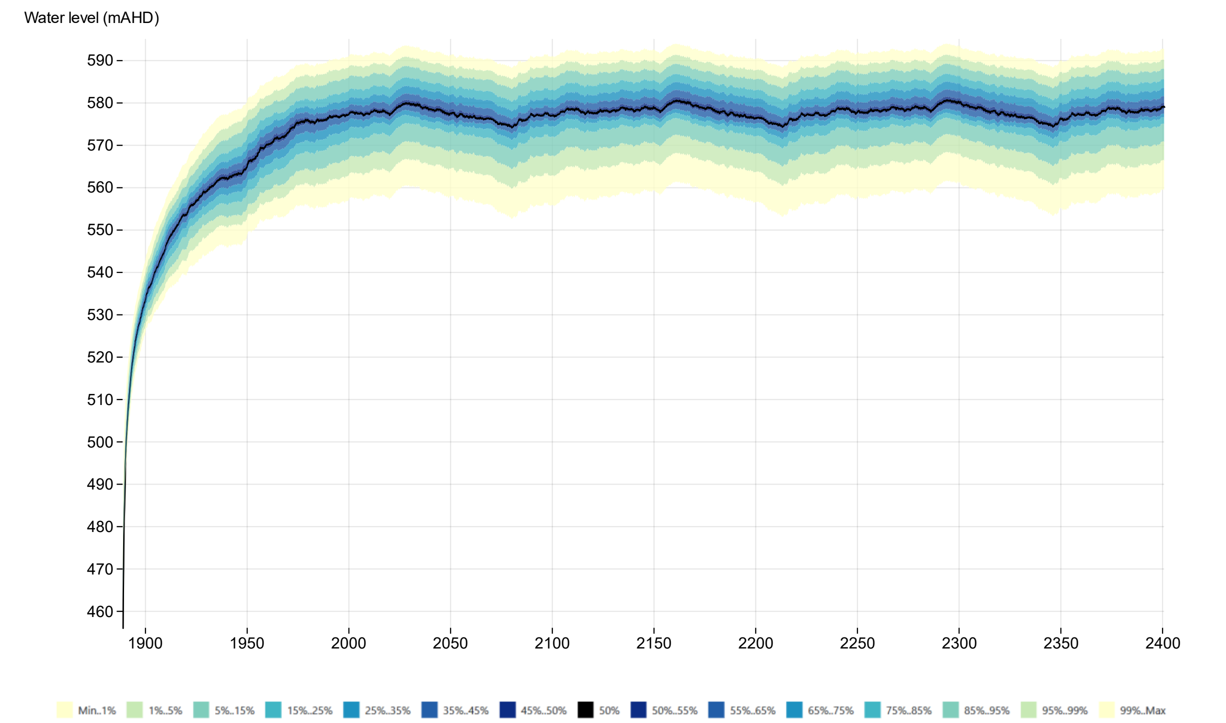

Figure 6
Results of Monte Carlo analysis – final void water level

Figure 7 shows the probability of exceedance of the peak water level calculated over each of the 5,388 realisations. This identifies a 50% probability that peak water levels would not exceed 580.7mAHD with a 95% probability (95^{th} percentile) of peak levels not exceeding 589.3mAHD. This means it is unlikely that peak lake levels would exceed 589.3mAHD as it represents a low (5%) probability outcome. It is noted that Jacobs (2022) had previously predicted through flow conditions would develop at 579mAHD. Based on **Figure 7**, the Final Void Water Balance Model Uncertainty Analysis identifies a greater than 50% probability of final void lake water levels exceeding 579mAHD.

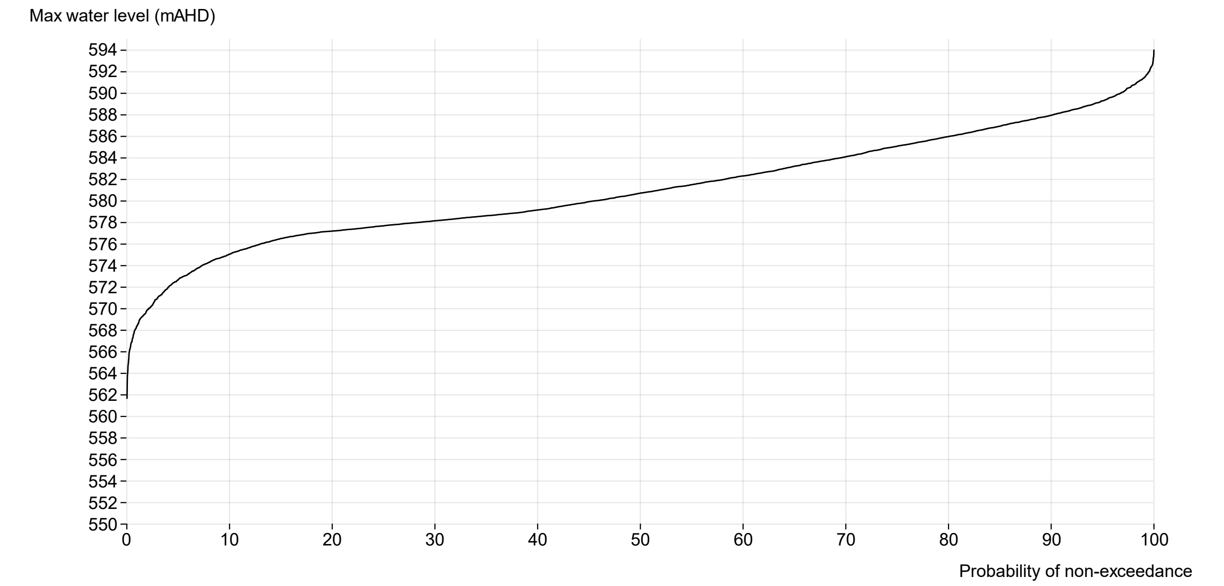

Figure 7
Probability of peak water level exceedance

95th Percentile Pit Lake Level: Representative Realisation

Realisation 3,158 was selected as being representative of the 95th percentile peak lake water level (589.3mAHD) as the parameters applied in this realisation were a close fit to most likely values applied in the Final Void Water Balance Model Uncertainty Analysis. **Figures 8** to **10** show the input parameters for this realisation compared to their respective PDF. It should be noted that other realisations, with differing combinations of input parameters, yield similar peak water levels.

Table 5 compares the average annual water balance for Realisation 3,158 to the previous model results (note that the tabulated EIS water balance model results were based on simulations starting at the equilibrium level – and therefore do not show a net inflow over time).

Table 5
Average annual water balance – Realisation 3,158 vs Previous Analysis

Item	EIS (Existing SILO)	EIS (HI.H Climate)	Realisation 3,158
Inflows	**ML/a**	**ML/a**	**ML/a**
Direct rainfall	188	188	234.9
Pit runoff	45	50	30.0
Rehabilitated surface runoff	-	-	6.1
Groundwater inflow	92	112	166.6
Total inflow	**325**	**350**	**437.7**
Outflows	**ML/a**	**ML/a**	**ML/a**
Pit evaporation	325	350	401.4
Total outflow	**325**	**350**	**401.4**
Net inflow (ML/a)	**0**	**0**	**36.3**
Annual volume increase (ML/a)	**0**	**0**	**36.3**

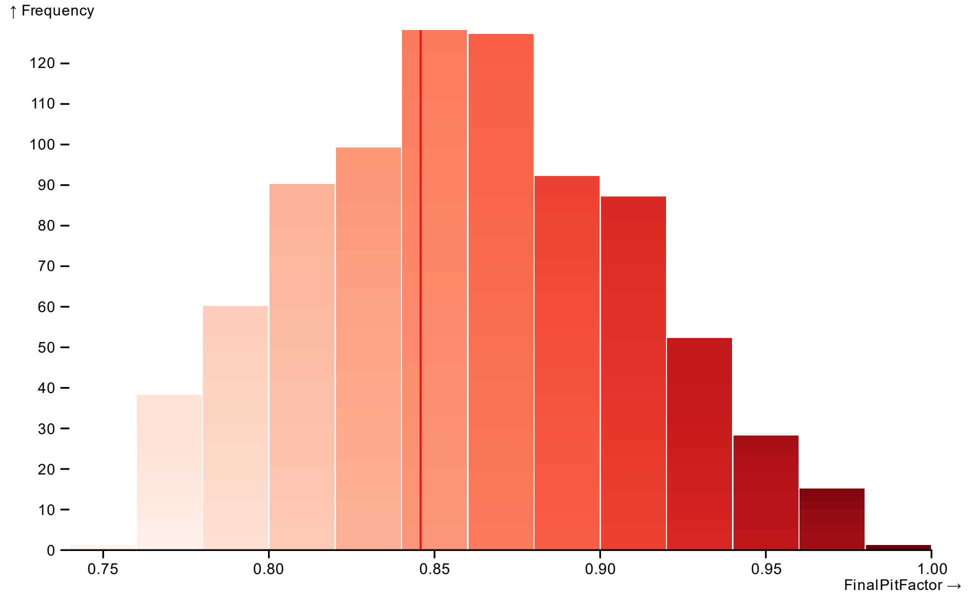

Figure 8
Modelled Pit Evaporation factor for Realisation 3,158 (red line) compared to PDF (at 589.3mAHD ± 5m)

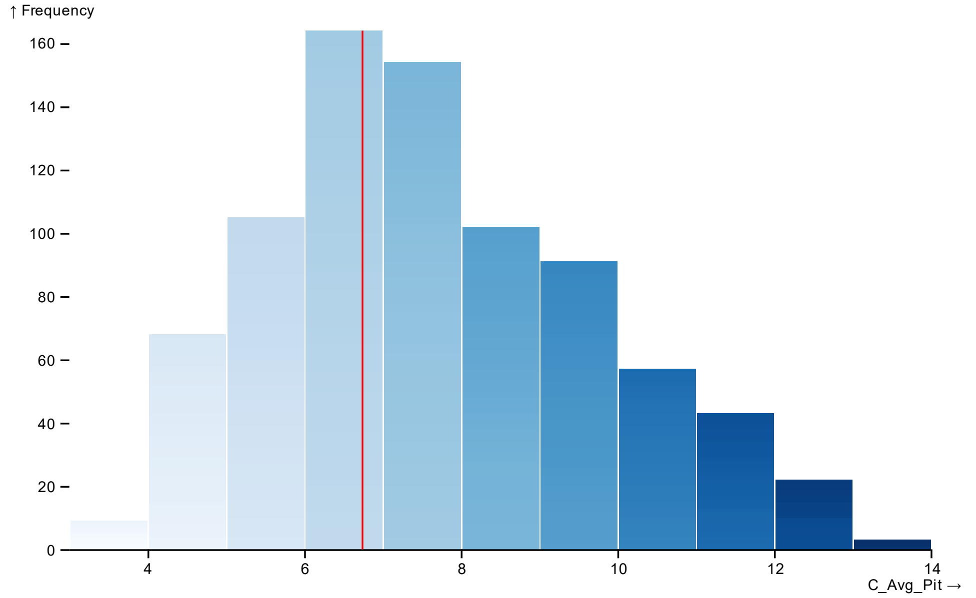

Figure 9
Modelled Pit Runoff C_{avg} for Realisation 3,158 (red line) compared to PDF

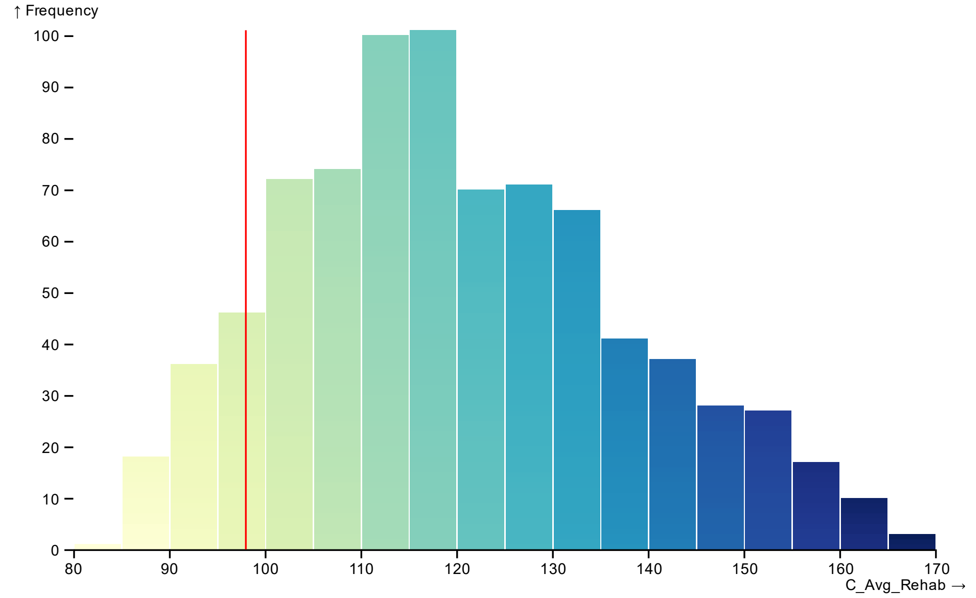

Figure 10
Modelled Rehab Runoff C_{avg} for Realisation 3,158 (red) compared to PDF

4 Testing Final Void Behaviour

4.1 Methodology

4.1.1 Introduction

The behaviour of the final void in the groundwater setting based on the pit lake water level time series resulting in the 95th percentile peak water level (Realisation 3,158) was assessed using the EIS groundwater model. This model was updated with the parameters from the groundwater uncertainty modelling realisation (Model Run 288) that provided the stage-inflow curve used as input for Realisation 3,158. The groundwater model was then run in transient mode with particle tracking applied to assess the potential for seepage and pathways from the final void. Once results had been reviewed, another model run was conducted with a simple mitigation option applied.

4.1.2 Updates to the Groundwater Model

The following changes were implemented to the EIS groundwater model to assess the implications on the local groundwater setting from the pit lake water level time series output from Realisation 3,158.

Modifications to Model Hydraulic Parameters

Hydraulic conductivity, storage and recharge zones and parameters were updated to those utilised in Model Run 288. A summary of the parameters from this realisation are provided in **Table 6**.

Table 6
Updated Hydraulic Parameters – Model Run 288

Parameter	Min	Max	Mean
Horizontal hydraulic conductivity (m/day)	3.28×10^{-5}	2.92×10^{1}	6.89×10^{-1}
Horizontal to vertical hydraulic conductivity ratio	0.001	1.000	0.040
Specific storage (m-1)	2.6×10^{-6}	8.38×10^{-3}	5.2×10^{-4}
Specific yield (%)	0.3%	39.9%	5.9%
Rainfall recharge (mm/day)	2.01×10^{-2}	1.36×10^{-1}	6.02×10^{-2}

Modifications to Boundary Conditions

a) Final Void

The final void was represented using a specified head boundary condition in model layers 1, 2, 3, 4 and 5. The specified heads were set commensurate with the outputs of Realisation 3158, representing the 95th percentile final void water level time series. The daily timestep pit lake level outputs of Realisation 3,158 were averaged to align with the 6-monthly timestep of the groundwater model.

b) Drain boundary conditions

All drain boundaries representing surface drainage features within the footprint of Waste Rock Emplacement were removed to reflect the final landform.

c) Recharge zones

Rainfall recharge zones and rates were modified to be consistent with those of Model Run 288.

4.1.3 Mitigation Measures

For the mitigation scenario, constructed wetlands (infiltration basins) were simulated on the down-gradient southwestern and southeastern margins of the final void. The infiltration basins were simulated as specified flux boundary conditions with the total flux being informed by the modelling of runoff contributions from upstream catchments. In reality, these infiltration basins would be developed as constructed wetlands, whereby they passively function without requiring ongoing monitoring or maintenance. Such features are commonly utilised in urban settings for passive treatment of stormwater runoff (i.e. bioretention basins [WaterbyDesign, 2014]).

As a mitigation measure, these infiltration basins would act as a localised source of enhanced groundwater recharge. This localised recharge would create a mounding response beneath the basin, reversing the hydraulic gradient and directing flow towards the final void. This would effectively restrict the potential for groundwater outflow from the final void.

To establish the likely runoff available to enter constructed wetland and therefore the likely rate of seepage available for groundwater modelling, WRM simulated upstream catchment runoff to develop a seepage timeseries that was provided as input to the groundwater modelling of infiltration as enhanced recharge. Runoff entering the wetlands was estimated using the AWBM developed for the EIS and the contemporised SILO climate dataset (refer Section 3.1.2). The average volume of seepage is approximately 0.182ML/day but would naturally vary over time with varying rainfall.

The contributing catchments providing runoff to the infiltration basins were modelled with the following characteristics and are shown on **Figure 11**.

- Eastern wetland:
  - 150ha natural catchment
  - 28.2ha rehabilitated catchment
- Western wetland:
  - 37ha natural catchment
  - 0ha rehabilitated catchment

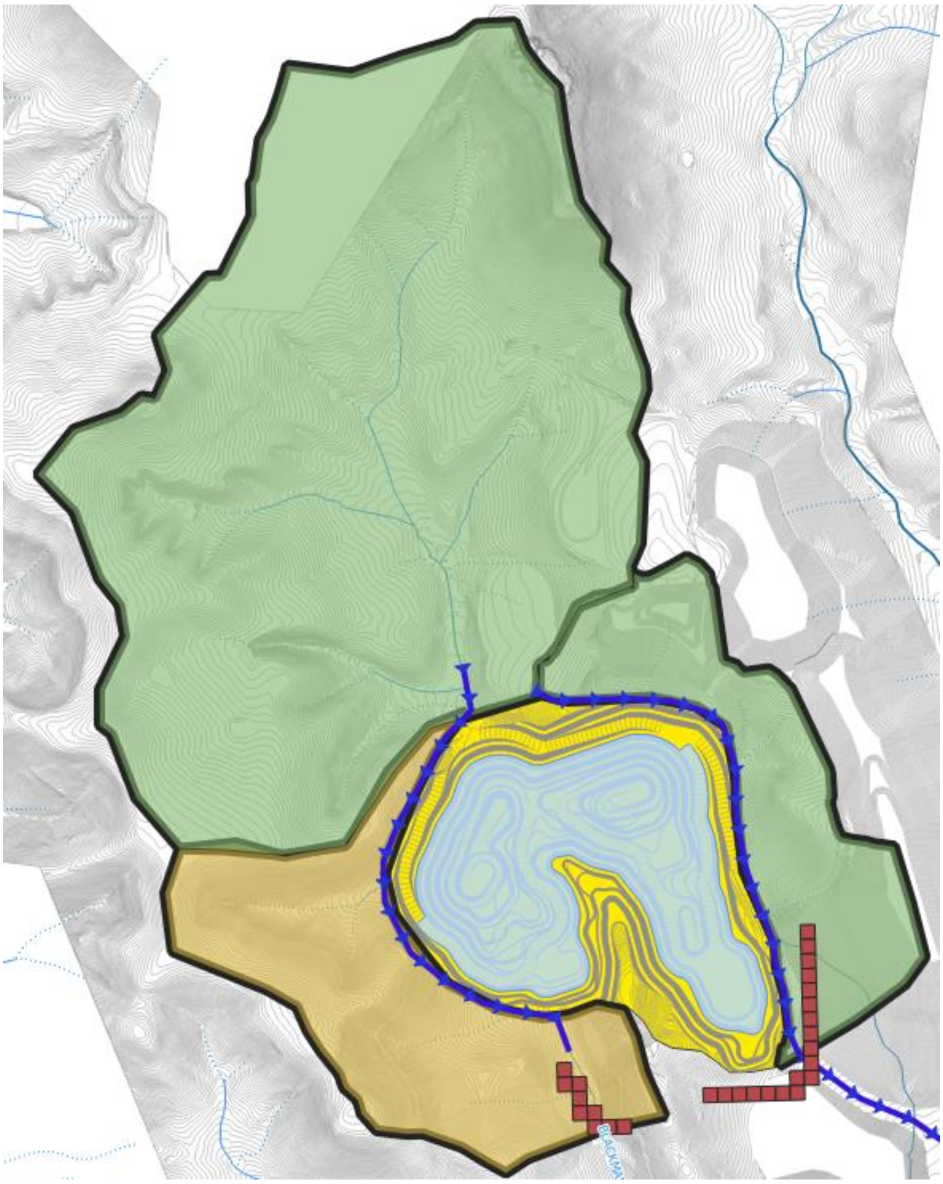

Figure 11
Proposed constructed wetlands – augmented eastern wetland

4.2 Particle Tracking Outcomes

Particle tracking for the unmitigated 95th percentile peak water level time series (Realisation 3,158) indicates a potential for seepage from the final void to reach Hawkins Creek following equilibrium. Travel times for seepage are relatively slow, in the order of 100 to 200 years following equilibration, with the longer travel times occurring from the southwestern section of the final void. The groundwater gradient adjacent to the final void, in areas of potential outflow would also be relatively low (between 0.0051 and 0.0161) with the average groundwater gradient between final void and Hawkins Creek would be 0.02. With the inclusion of infiltration basins as a passive mitigation measure, the modelling identifies that particles escaping from the final void are effectively stopped.

Figure 12 and **Figure 13**, below, show 1,000-year particle traces for the unmitigated and mitigated scenarios respectively. For the unmitigated scenario, particles are observed to reach Hawkins Creek, with one trace (orange line) travelling beneath, but not intercepted by, Lawsons Creek. For the mitigated scenario, after 1,000 years all particles remain effectively constrained within the final void, with only one trace (red line in **Figure 13**) travelling only metres from the final void in that time. The configuration of the mitigated particle tracking model, including the locations of modelled infiltration basins and particle seed points (origins), is shown on **Figure 14**.

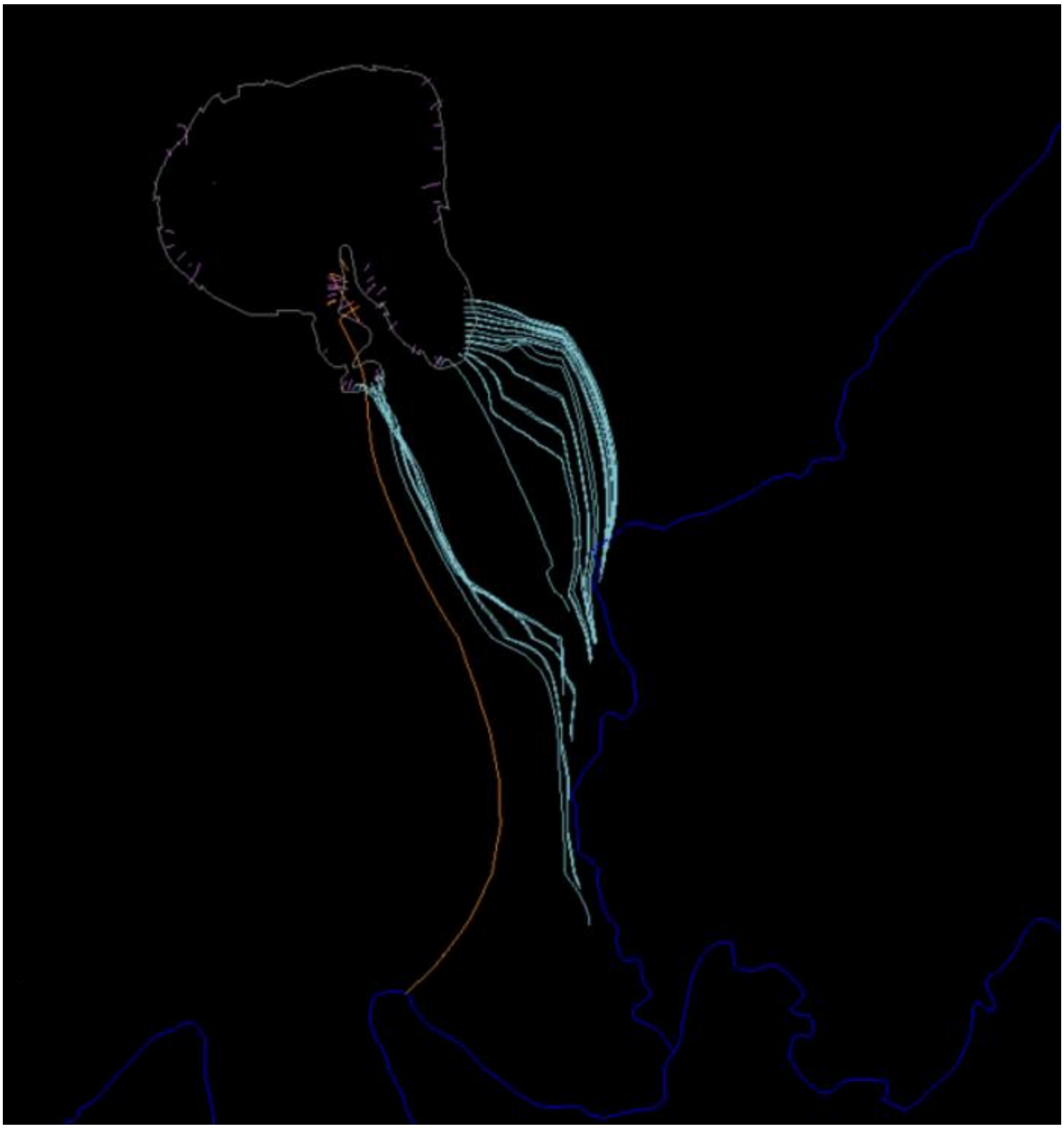

Figure 12
95th Percentile Final Void Pit Lake Water Levels – Unmitigated Particle Tracking

Figure 13
95th Percentile Final Void Pit Lake Water Levels – Mitigated Particle Tracking

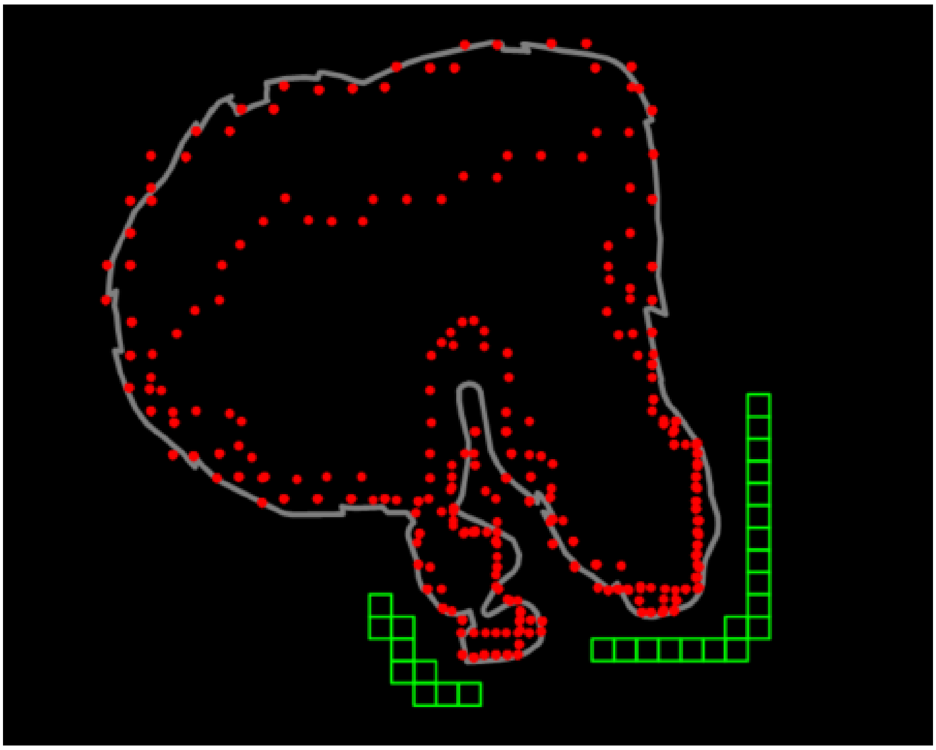

Figure 14
Modelled Infiltration Basin Locations and Particle Seed Points

5 Reasonable Mitigation Measures

5.1 Constructed Wetlands (Infiltration Basins)

Constructed wetlands are commonly adopted features in water sensitive urban design that collect stormwater runoff for passive treatment (sediment, nutrient, metals and hydrocarbon removal) to achieve improved urban water quality outcomes. However, constructed wetlands also create a point source location for enhanced recharge to the local groundwater setting. In the case of the final void, a constructed wetland at key locations and the recharge it would create would locally reverse hydraulic gradient back towards the open cut pit.

As noted in Section 4.1.3, AWBM runoff time series from upstream catchments (refer **Figure 11**) were provided by WRM to Jacobs as input for modelling. This modelling situated infiltration basins / constructed wetlands southeast and southwest of the open cut pit to assess their ability to limit outflow from the final void pit lake. Jacobs then modelled the 95th percentile peak water level time series output of Realisation 3,158 to identify that this measure provides effective mitigation, even for low probability pit lake water level outcomes.

Based on modelling undertaken by Jacobs and described in Section 4.2, constructed wetlands provide a technically feasible option to limit outflow from the final void pit lake.

5.2 Final Void Geometry

Once the groundwater setting reaches post-mining equilibrium, climatic conditions become the dominant influence on final void pit lake level behaviour. This is because pit lake water levels and thus groundwater inflows, will be determined by the balance between direct rainfall and catchment runoff inflows and evaporative losses. As the average evaporation rate significantly exceeds that of rainfall and, by default, runoff, pit lake water levels could be reduced by modifying final void geometry to increase pit lake surface area.

WRM investigated the sensitivity of peak pit lake water levels to increasing evaporative surface area and using the 0.85 top of pit evaporation factor of Realisation 3,158. **Figure 15** shows the results of this analysis that identifies a near linear relationship between peak pit lake level and additional lake surface area. This means that for every additional hectare of lake surface area peak pit lake water levels would be reduced by approximately 0.55m.

The amendment of final void geometry is technically feasible and would not necessarily require an increase to Project-related disturbance. Whilst amending final void geometry may provide full mitigation against outflow from the pit lake by depressing pit lake water levels, it is possible that this option could be utilised in concert with other options to provide additional contingency for mitigation.

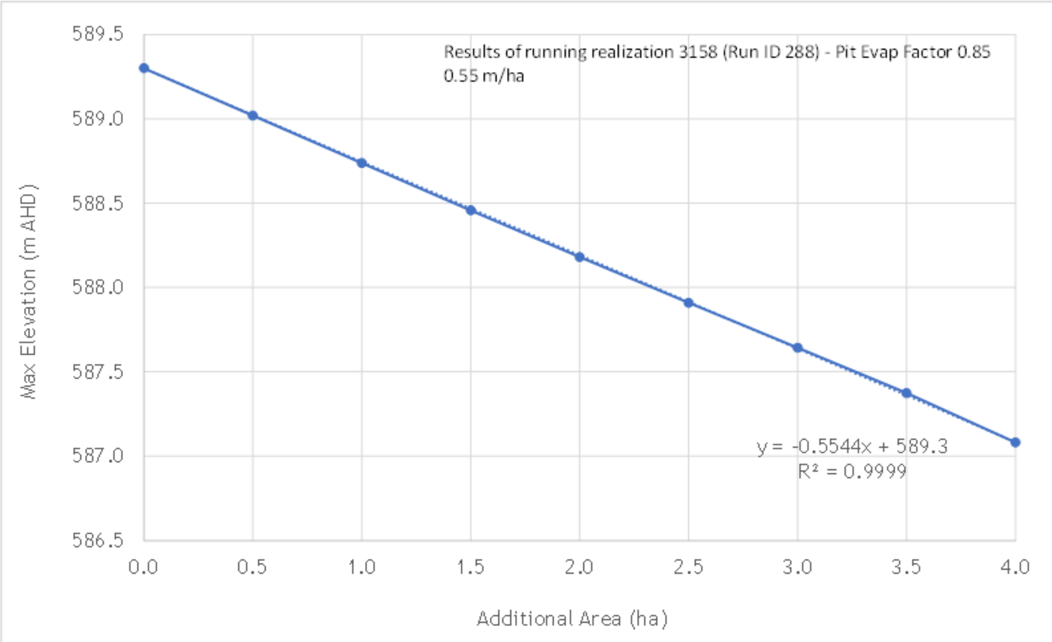

Figure 15
Relationship Between Maximum Pit Lake Water Level and Pit Lake Evaporative Surface Area (from Realisation 3,158)

5.3 Grout Injection

Grout injection is widely used in mining and other engineering applications as a groundwater control practice with the potential to significantly reduce the rate of groundwater inflow to the final void. As the open cut pit is developed during mining operations, areas of faulting or fracturing within the pit wall that are associated with elevated hydraulic conductivity and groundwater inflow would be easily identified. On the completion of mining activities and with groundwater level recovery, these same high yielding zones would then transmit groundwater inflow to the final void.

Drilling into identified zones and injecting grout into the fractures would significantly reduce the bulk hydraulic conductivity of the formation. This would reduce groundwater inflows to the final void post mining, especially once dynamic equilibrium levels are reached, and therefore reduce peak pit lake water levels.

The approach to grouting would need to be specific to the structures identified during operations and also consider the potential implications for pit wall depressurisation and slope stability. However, with suitable planning and implementation, the grouting of high yielding zones in the pit wall represents a simple, technically feasible and effective method to reducing groundwater inflow to the final void. By reducing groundwater inflows, pit lake water levels will also be reduced, thus reducing the potential for outflow from the final void pit lake.

The injection of grouting is unlikely to provide full mitigation on its own, but it could be utilised in concert with other options to provide additional contingency for mitigation. As noted in Section 3.1.3, at an elevation of 575mAHD, the median inflow from the Groundwater Model Uncertainty Analysis is 0.48ML/day, compared to the previously adopted 0.2ML/day. In the eventuality that this magnitude of inflow is realised, grouting has the potential to significantly reduce groundwater inflow to a point where throughflow conditions are averted.

6 Uncertainty Analysis Modelling vs EIS Groundwater Modelling

The Groundwater Modelling Uncertainty Analysis typically resulted in higher final void stage-inflows and consequently resulted in elevated pit lake water levels compared to those predicted by the EIS groundwater model. Key differences in the approach to the Uncertainty Analysis modelling and the EIS modelling are noted below.

Uncertainty analysis is a useful tool for informing relative risk associated with mining operations, particularly in high-risk environments where hydrogeological conditions are not well understood. The uncertainty analysis performed for this study randomly selected combinations of hydraulic parameters (horizontal hydraulic conductivity, vertical hydraulic conductivity via Kh/Kz ratio, recharge, and storage parameters) from a broad range of plausible values. Multiple model realisations were then run using these randomly selected hydraulic parameters and results assessed based on predetermined calibration criteria. The results of model runs meeting the calibration criteria were then collated as a group and processed to establish their probabilistic distribution. For this study, the subject of interest was limited to final void groundwater inflows.

In contrast, parameterisation of the EIS groundwater model was informed by hydraulic testing within the Mine Site and refined through calibration to local and regional groundwater levels. As documented in Section 4 of (Jacobs, 2022) the following hydraulic testing has occurred within the Mine Site:

- 36 hydraulic (slug) tests, providing estimates of formation hydraulic conductivity;
- Eight airlift recovery tests, providing qualitative yield assessment and estimates of formation hydraulic conductivity;
- 21 packer injection tests, providing estimates of formation hydraulic conductivity;
- Six short term pumping tests (2 to 4 hours), providing estimates of formation hydraulic conductivity;
- Two long-term pumping tests (3 days), providing estimates of formation hydraulic conductivity and aquifer storage coefficients; and
- One period of extended pumping (approximately 3 months) with extensive groundwater level observation across the Mine Site, allowing refinement of calibrated model hydraulic conductivity and storage parameters within the mining area.

These investigations provide over 70 individual assessments of formation hydraulic properties within the Mine Site which is the primary area of interest with respect to constraining groundwater inflow to the open cut pit during mining operations.

It is further noted that the lower groundwater inflows predicted by the EIS groundwater model are also consistent with previous investigations undertaken for the Project (and its earlier predecessors)[3] which have all identified low groundwater yields and limited aquifer potential as possible limitations with respect to Project water supply and associated groundwater inflows to mining operations.

[3] Coffey (1998). Hydroilex (2003), Jewell (2003), Merrick (2011), SKM (2013), Jacobs (2014) – refer to EIS groundwater report for references.

7 Discussion

The Uncertainty Analysis has identified that at higher pit lake levels, through flow conditions may develop in some sections of the void. Modelling of the 95th percentile (low probability) final void water level scenario demonstrates that successful mitigation can be achieved using passive measures. Such measures would also provide readily achievable mitigation in higher probability (i.e. more likely) scenarios that result in lower pit lake water levels than predicted under the Final Void Water Balance Model Uncertainty Analysis. Modelling of final void behaviour using the outcomes of the Final Void Water Balance Model Uncertainty Analysis has served to demonstrate that, even in a low probability through flow scenario:

- the groundwater gradient adjacent to the final void, in areas of potential outflow would be relatively low (between 0.0051 and 0.0161);
- the average groundwater gradient between final void and Hawkins Creek would be 0.02;
- following equilibrium, travel time to Hawkins Creek would be in the order of 100 to 200 years).

Given that the final void lake would be present in perpetuity and that evapoconcentration of salts, acids and metals may occur over time, Bowdens Silver has committed that the final landform would incorporate passive controls that restrain or remove the occurrence of through flow.

This analysis has successfully tested the implementation of constructed wetlands in isolation. In practice there would be other options available for consideration, assessment and development over the Project-life. Other options that could be assessed during mining and as part of final void management plan investigations include, but are not necessarily limited to the following.

- Mine plan modification to amend final void geometry and maximise the pit lake surface area available to evaporation, thus lowering pit lake water levels at equilibrium.
- Grouting of high yielding zones encountered during mining. This would act to lower bulk formation hydraulic conductivity, reducing inflow to the final void post mining and lowering pit lake water levels at equilibrium.

Predictive analysis of final void behaviour undertaken for the EIS was informed by hydraulic testing within the Mine Site and updated on several occasions to refine the assessment in response to comments provided by NSW Government agencies. Bowdens Silver maintains the position that the most likely outcome for the final void is that it would remain in the local groundwater setting as a terminal sink.

Planning for Mine closure would involve updates to the groundwater modelling based on actual groundwater inflow data collected during mining operations. This data would be supplemented by data collected to calibrate the site water balance model (i.e. runoff and evaporation). The assessment of the magnitude of groundwater inflows to the final void will thus be refined as mining proceeds below the water table and active dewatering is required. This would provide time for the refinement of groundwater modelling and further assessment of final void behaviour and pit lake water levels. This would then be used in the design and implementation of mitigation measures if required.

Based on hydraulic testing undertaken at the Mine Site to date, it is anticipated that the groundwater model used for the EIS applied conservative estimates for groundwater inflow to the final void. Therefore, it is critical that final Mine closure plans are informed by actual records of groundwater inflows to the open cut pit that are used to verify the modelled parameters of the local groundwater setting. The process and timing for groundwater model updates would be presented in a Water Management Plan for the Project which would be prepared in consultation with DPE Water and approved for implementation by DPE. It is currently envisaged that the groundwater modelling would be updated within two years of mining intercepting the regional aquifer. Throughout the life of Mine, annual reporting would include a comparative assessment of observational results and model predictions to ensure the groundwater model remains representative of the groundwater setting. A further review of the groundwater model would be undertaken prior to Mine closure.

8 References

Barnett, B., Townley, L.R., Post, V., Evans, R.E., Hunt, R.J., Peeters, l., Richardson, S., Werner, A.D., Knapton, A., and Boronkay, A. 2012. *Australian groundwater modelling guidelines.* Sinclair Knight Merz and National Centre for Groundwater Research and Training. Waterlines Report Series No. 82, June 2012.

Doherty, J., 2015. *Calibration and Uncertainty Analysis for Complex Environmental Models.* Watermark Numerical Computing, Brisbane, Australia. ISBN: 978-0-9943786-0-6.

Doherty, J., 2016. PLPROC: *A parameter list processor. Software manual*.

HydroAlgorithmics, 2019. AlgoCompute web site, https://www.algocompute.com/. Accessed 16 September 2022.

Jacobs Group (Australia) Pty Limited, 2022. *Bowdens Silver Updated Groundwater Assessment. Report* IA132500 for Bowdens Silver Pty Limited, February 2022.

McJannet, D.L., Webster, I.T., and Cook, F.J. , 2012. *An area-dependent wind function for estimating open water evaporation using land-based meteorological data. Environ. Modell. Software 31, 76–83.*

McJannet, D., Hawdon, A., Boadle, D., Baker, B., van Neil, T., Littleboy, A., Trefry, M., Rea, I. and Fandrich, R, 2016. *Measurements and modelling of evaporation from abandoned mine pit lakes. AusIMM - Life-of-Mine 2016, Brisbane, Australia.*

McJannet, D., Hawdon, A., Van Niel, T., Boadle, D., Baker, B., Trefry, M., Rea, I. and Fandrich 2017. *'Measurements of evaporation from a mine void lake and testing of modelling approaches' Journal of Hydrology 555 (2017) 631–647.*

McJannet, D., Hawdon, A., Baker, B., *Ahwang, K., Gallant, J., Henderson, S. & Hocking, A.* 2019, *'Evaporation from coal mine pit lakes: measurements and modelling', in AB Fourie & M Tibbett (eds), Mine Closure 2019: Proceedings of the 13th International Conference on Mine Closure, Australian Centre for Geomechanics, Perth, pp. 1391-1404, https://doi.org/10.36487/ACG_rep/1915_109_McJannet.*

Merrick, D. and Merrick, N. (2015). *AlgoMesh: A new software tool for building unstructured grid models*. In Proc. MODFLOW and More, Golden, Colorado.

Merrick, D. (2017). *AlgoCompute: Large-scale calibration and uncertainty analysis made easy in the cloud*. In Proc. MODFLOW and More, Golden, Colorado.

Miller, K.L., Berg, S.J., Davison, J.H., Sudicky, E.A., Forsyth, P.A. (2018). *Efficient uncertainty quantification in fully-integrated surface and subsurface hydrologic simulations*. Advances in Water Resources, Volume 111, pp. 381-394.

Mood, A.M., Graybill, F.A., Boes, D.C. (1974). *Introduction to the Theory of Statistics*, 3rd Edition. Mcgraw-Hill, Inc. ISBN: 978-0-07-042864-5.

Morton, F I, 1983. *Operational estimates of areal evapotranspiration and their significance to the science and practice of hydrology, Journal of Hydrology, Volume 66, 1-76.*

Morton, Goard, and Piwowar, 1985. *Operational estimates of areal evapotranspiration and lake evaporation – Program WREVAP, NHRI paper No 24, Inland Waters Directorate, Environment Canada, Ottawa, 1985.*

PPK, 2002. *ACARP Project No C7007 Water Quality and Discharge Predictions to Final Void and Spoil Catchments, PPK Environment & Infrastructure, May 2002.*

Vrugt, J.A., ter Braak, C J.F., Diks, C.G.H., Higdon, D., Robinson, B.A., and Hyman, J.M. (2009). *Accelerating Markov chain Monte Carlo simulation by differential evolution with self-adaptive randomized subspace sampling*. International Journal of Nonlinear Sciences and Numerical Simulation, Volume 10, Issue 3, pp. 273-290.

WaterbyDesign (2014). *Bioretention Technical Design Guidelines.*

WRM Water and Environment Pty Ltd (WRM) (2022). *Updated Surface Water Assessment.* Presented as Appendix 3. Prepared on behalf of Bowdens Silver Pty Limited

Appendices

Appendix 1 Convergence of Groundwater Model Uncertainty Analysis

Appendix 2 Derivation of Pit Lake Evaporation Factors

Appendix 1

Convergence of Groundwater Model Uncertainty Analysis

(Total No. of pages including blank pages = 5)

A1.1 Convergence

In this section, charts are presented illustrating the convergence of the random sampling process for inflows at a sequence of pit lake stages[4]. Two types of chart are presented. The first shows the inflows at 10^{th}, 33^{rd}, 50^{th}, 67^{th} and 90^{th} percentiles as they evolve with the number of runs evaluated. The second shows the 10^{th}, 50^{th} and 90^{th} percentile values surrounded by their computed 99.7% confidence intervals, also as they evolve with respect to the number of runs evaluated. Note that 33^{rd} and 67^{th} percentile confidence intervals have been omitted from these charts to ease readability; the intervals in these cases were similar or narrower in width than those of the 10^{th}, 50^{th} and 90^{th} percentiles shown.

Percentile results were calculated from the LHS outputs strictly on a conservative "round to higher value" basis, and are represented as "probabilities of exceedance" in five categories: "very likely (90%) - **green**, "likely (67%)" - **light yellow-green**, "about as likely as not (50%)" - **black**, "unlikely (33%)" - **orange**, and "very unlikely (10%)" - **red**.

To clarify, a "very unlikely (10%)" probability of exceedance value of X for a metric should be interpreted as "10% of realisations from the set of accepted realisations resulted in a value for this metric larger than X."

Solid lines in the convergence charts represent the actual sampled percentile values, and dashed lines represent the 99.7% confidence intervals of the percentile corresponding to their colour.

[4] As approximated by the groundwater model prior to refined definition by the Goldsim process.

Inflows at 560mAHD

Figure 16 and **Figure 17** show the change in inflow percentiles at 560mAHD with respect to the number of runs evaluated. The 99.7% confidence intervals indicate that reported values are within 0.030ML/d of the true values with high probability. All 449 SRMS-accepted runs exhibited a 560mAHD stage.

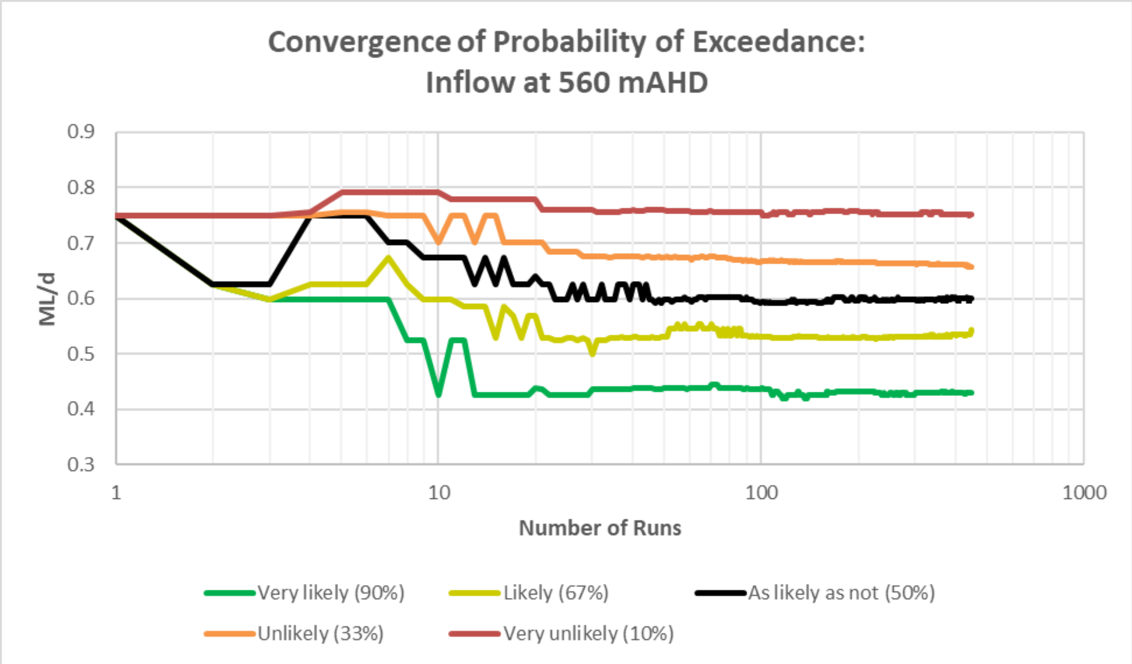

Figure 16
Change in Inflow Percentiles with Number of Model Runs at a Pit Lake Stage of 560mAHD

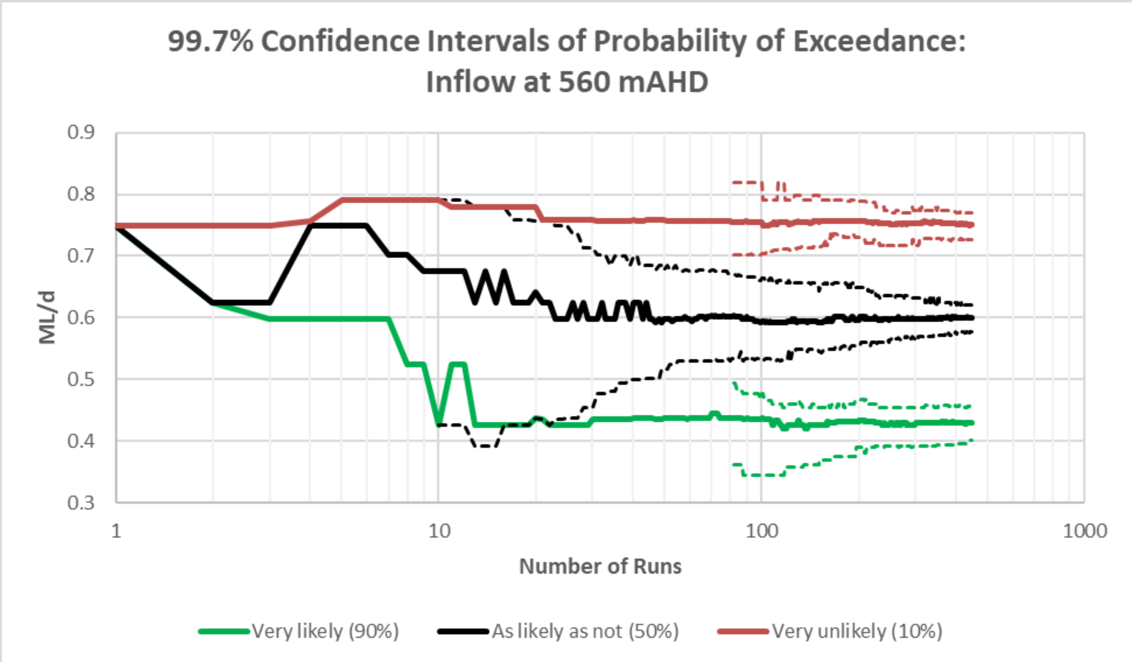

Figure 17
99.7% Confidence Intervals for Inflow Percentiles at a Pit Lake Stage of 560mAHD

Inflows at 579mAHD

Figure 18 and **Figure 19** show the change in inflow percentiles at 579mAHD with respect to the number of runs evaluated. The 99.7% confidence intervals indicate that reported values are within 0.034ML/d of the true values with high probability. All 449 SRMS-accepted runs exhibited a 579mAHD stage.

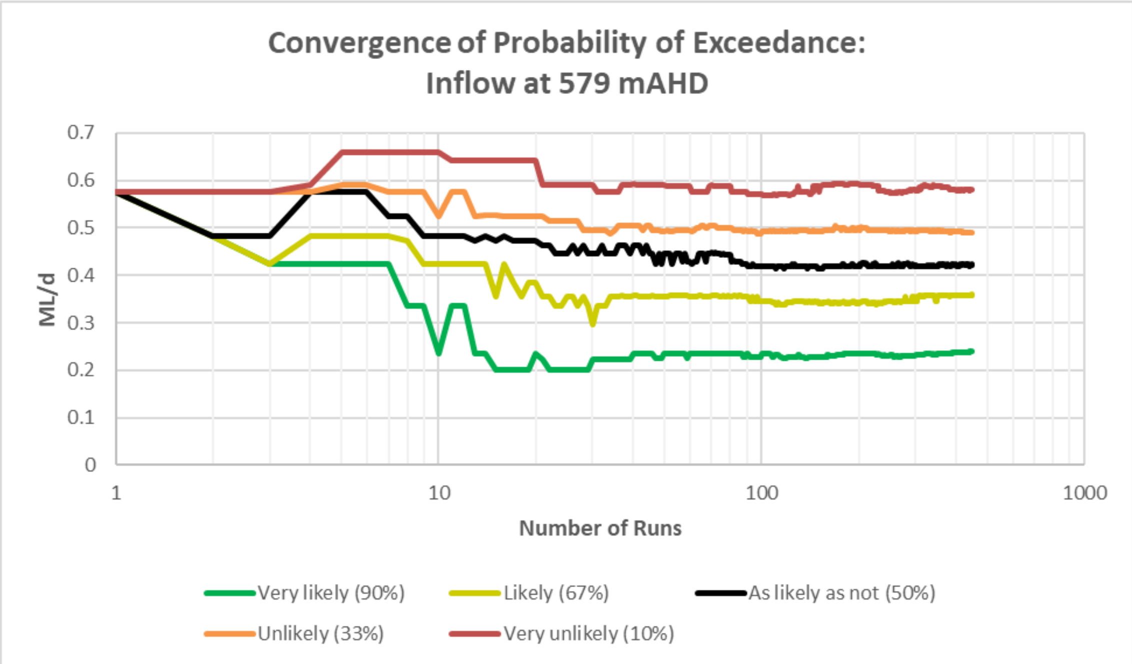

Figure 18
Change in Inflow Percentiles with Number of Model Runs at a Pit Lake Stage of 579mAHD

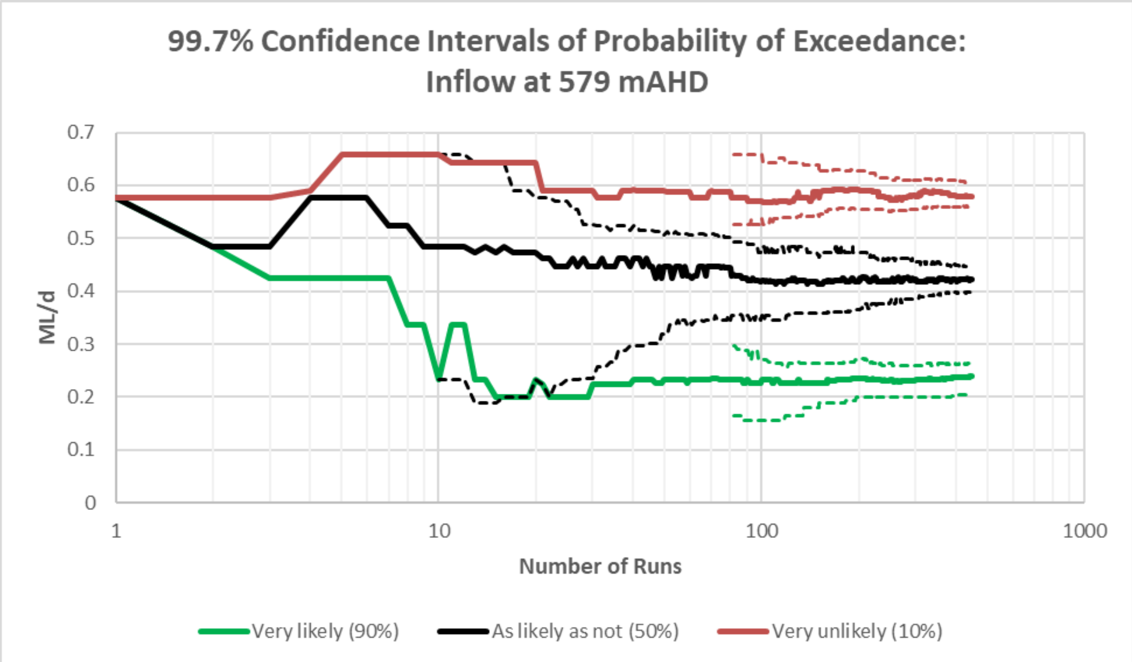

Figure 19
99.7% Confidence Intervals for Inflow Percentiles at a Pit Lake Stage of 579mAHD

Inflows at 590mAHD

Figure 20 and **Figure 21** show the change in inflow percentiles at 590mAHD with respect to the number of runs evaluated. The 99.7% confidence intervals indicate that reported values are within 0.032ML/d of the true values with high probability. 415 of the SRMS-accepted runs exhibited a 590mAHD stage.

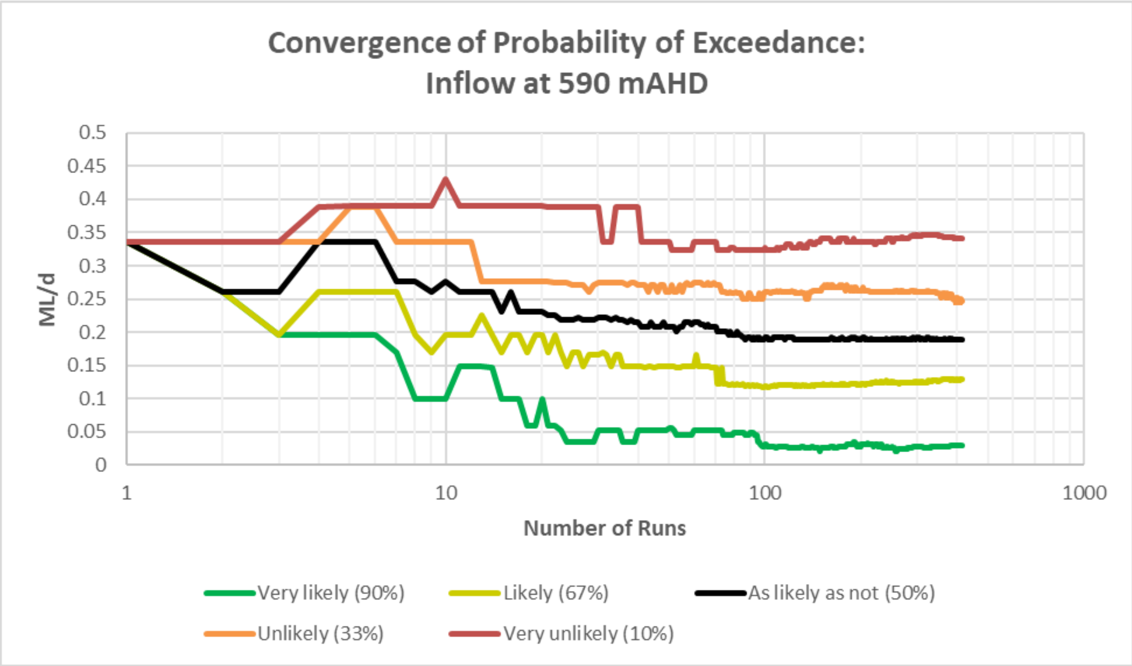

Figure 20
Change in Inflow Percentiles with Number of Model Runs at a Pit Lake Stage of 590mAHD

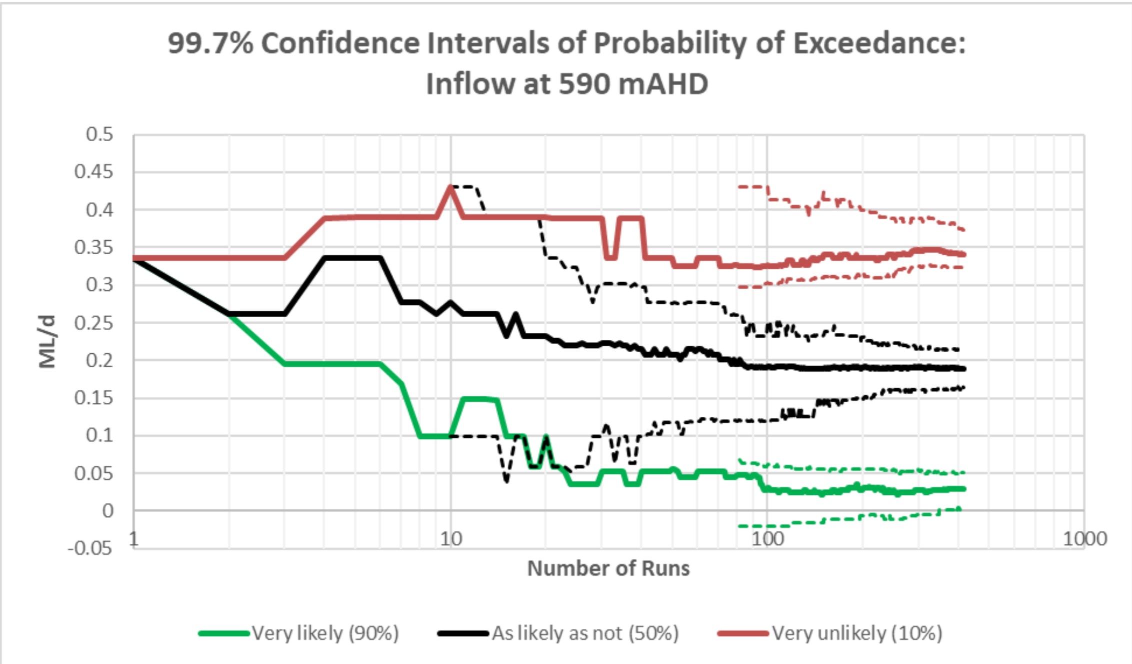

Figure 21
99.7% Confidence Intervals for Inflow Percentiles at a Pit Lake Stage of 590mAHD

Appendix 2

Derivation of Pit Lake Evaporation Factors

(Total No. of pages including blank pages = 6)

A2.1 Top-of-pit Lake Factor

The top-of-pit lake factor was sampled from a near symmetrical triangular distribution based on the results of studies of lake evaporation (Morton, Goard, and Piwowar, 1985). The factors were first adjusted to account for the use of Morton's Shallow Lake evaporation in the model (as opposed to Class A pan evaporation, which is commonly used for evaporation studies).

The resultant parameters are shown in **Table 7** and compared to the values used in the previous (WRM, 2022) analysis in **Figure 22**.

Table 7
Parameters Defining the Proposed PDF for the Top-of-pit Lake Factor

	Lower Limit	Most Likely	Upper Limit
Top-of-Pit Lake Factor	0.80	1.02	1.18
Equivalent Pan Factor	0.75	0.95	1.10

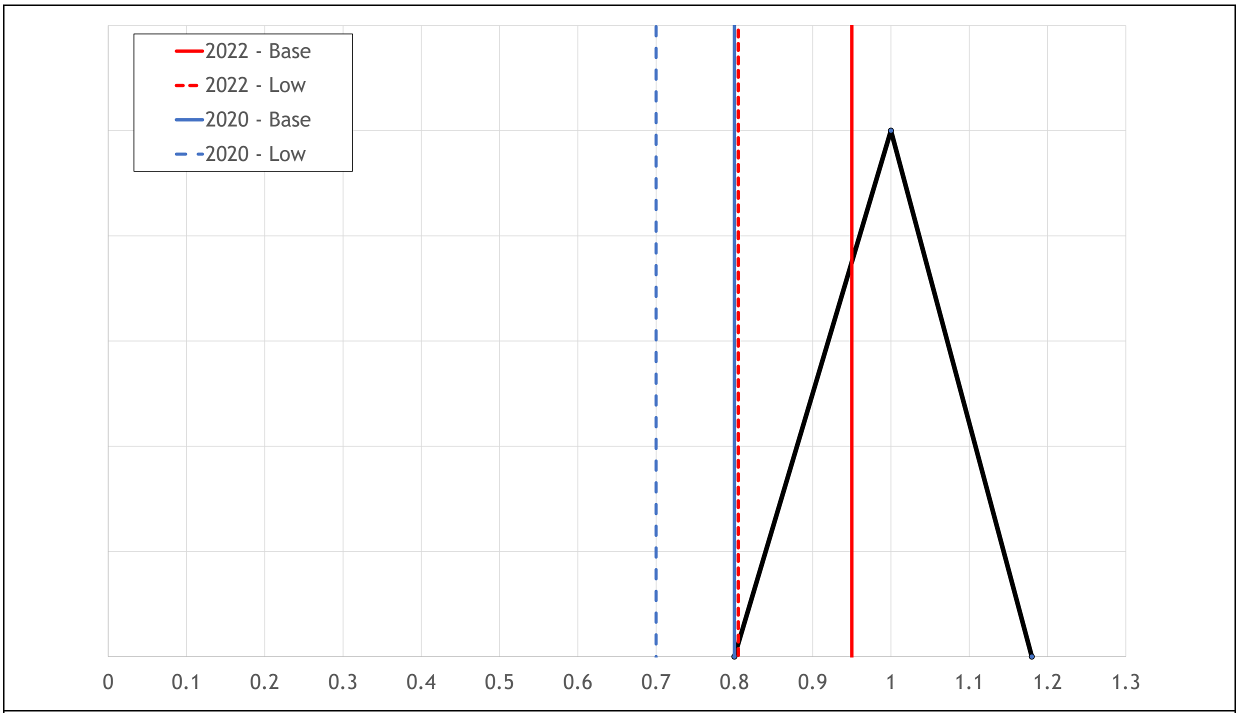

Figure 22
Top-of-pit PDF (black line) and previously adopted values

A2.2 Shading

In the CSIRO (McJannet et al, 2016) evaporation model, shading effects on the shaded pit lake surface are calculated by multiplying the solar radiation input by the average daily shortwave radiation ratio (SWRR). SWRR is the ratio of the total daily solar radiation input on the pit lake surface compared with that for an unshaded horizontal surface at this location.

Figure 23 shows the calculated SWRR for the Bowdens Final Void at various water levels. The effect is greatest in June, when the solar radiation input to the pit lake with a water level of 550mAHD is reduced by around 18%.

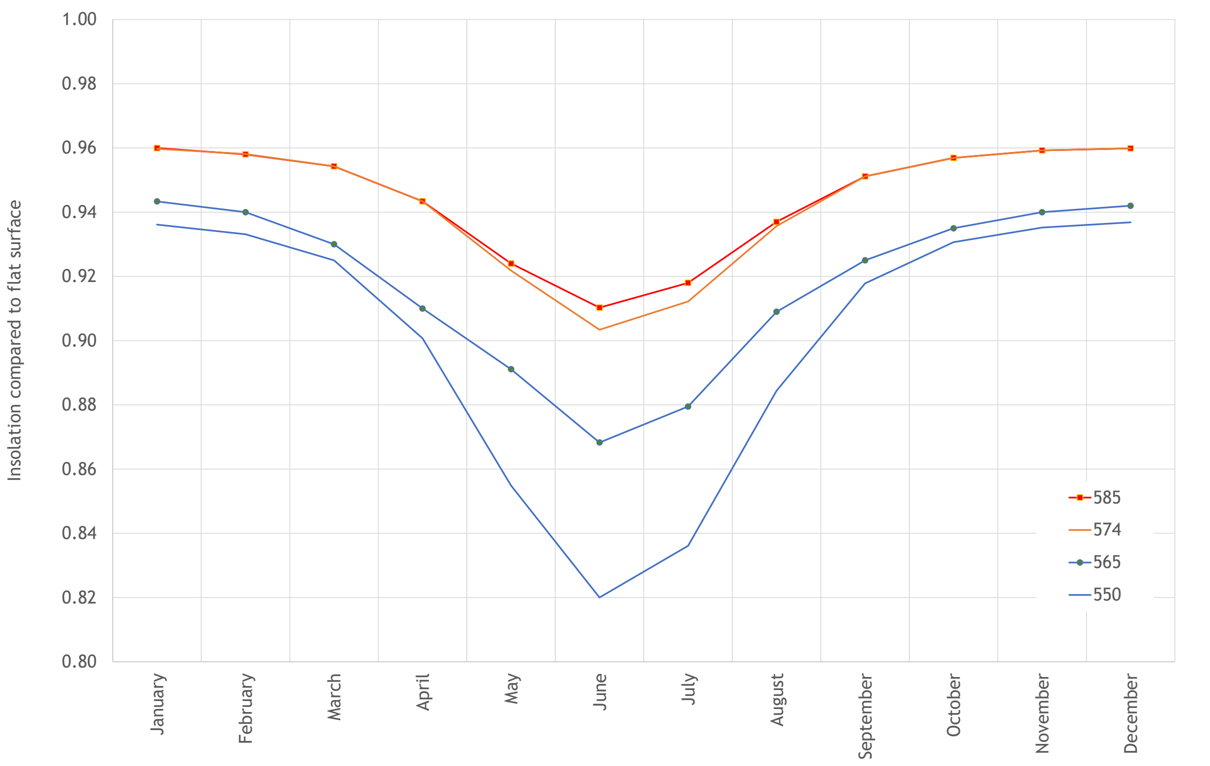

Figure 23
Monthly Variation in Shortwave Radiation at Various Water Elevations

At 574mAHD there would be a reduction in solar radiation of less than 6% for 75% of the year i.e. the effect of shading at Bowdens will be small - due largely to the shape of the void and the equilibrium water level.

The effect of the reduction in solar radiation on the evaporation rate was estimated from the Morton's shallow lake evaporation (applying the methodology used to derive the SILO data) – after scaling the solar radiation input by the SWRR. This resulted in average annual reductions in evaporation resulting from shading range from about 10% at 550mAHD to about 6% at 585mAHD. **Figure 24** shows the shading factors (ratios of shaded to unshaded Morton's shallow lake evaporation) derived from the analysis.

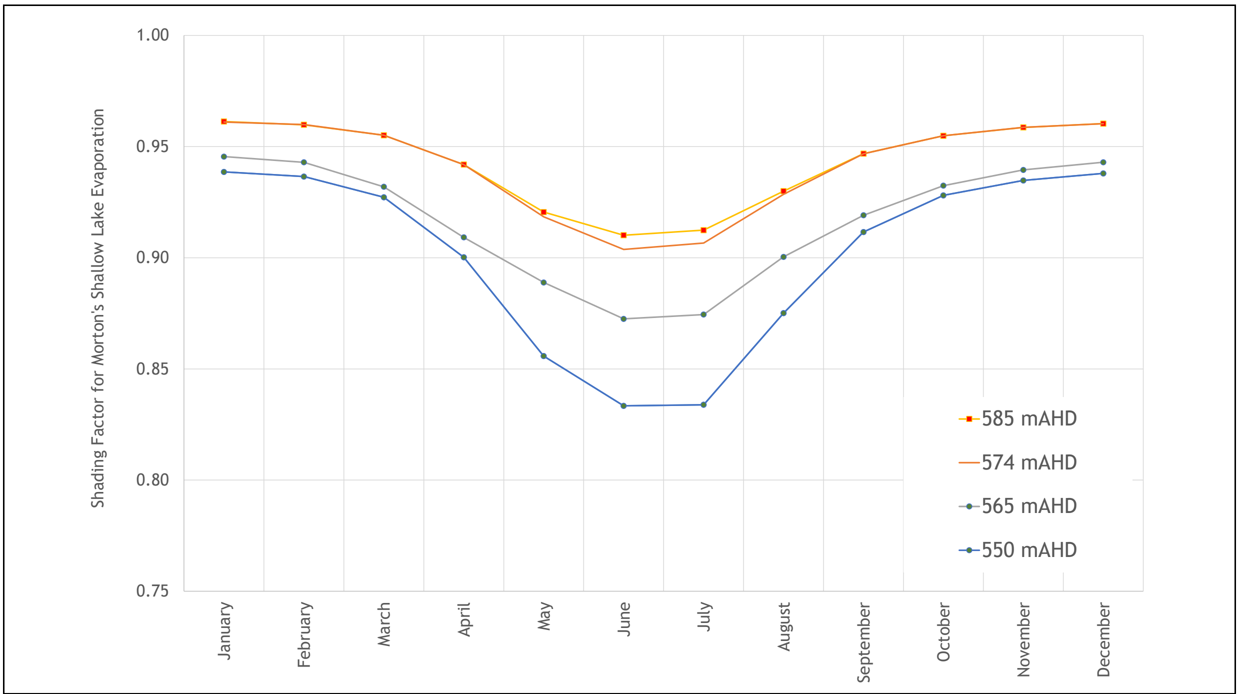

Figure 24
Shading Factors for Adjusting Morton's Shallow Lake Evaporation

For the Monte Carlo analysis, the daily evaporation rate will be adjusted for shading by applying annual shading factors interpolated (with water level) from the results of the above analysis. This adopted water elevation vs shading factor relationship is shown in **Figure 25**.

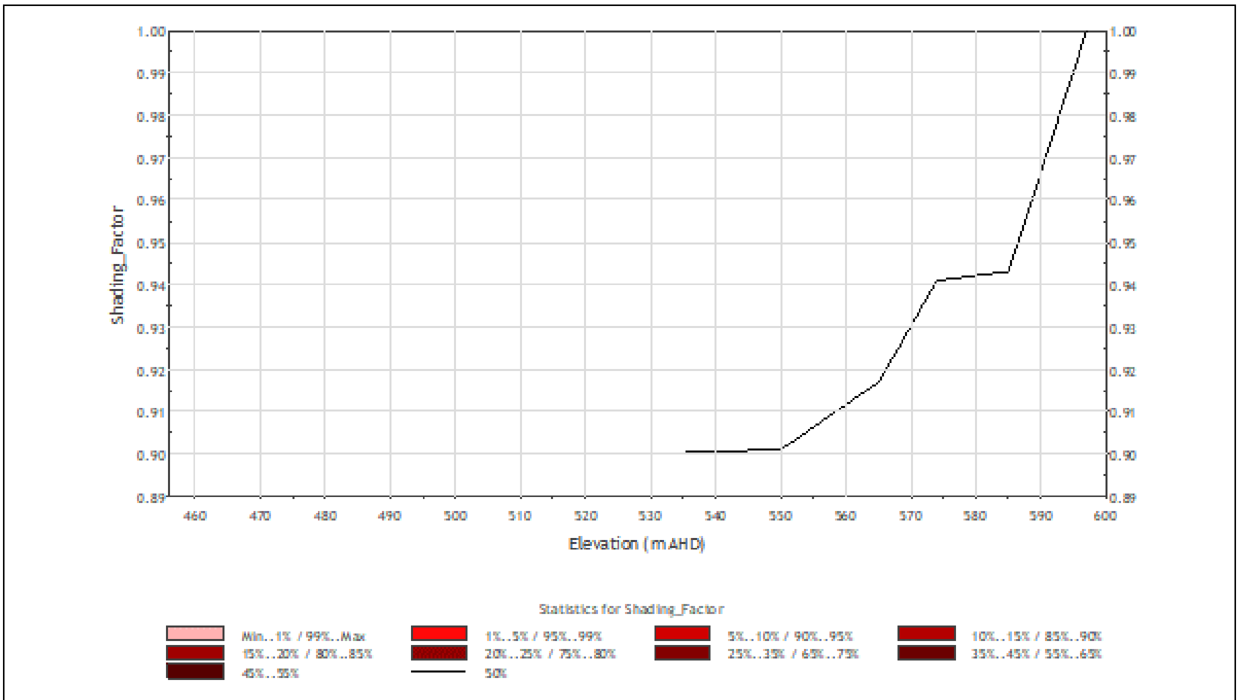

Figure 25
Shading Factor used to Produce Pit Factor over the Range of Elevations

The seasonal variation in the effects of shading was applied by interpolating between the seasonal curves (normalised to the mean annual factor) derived in **Figure 24**.

A2.3 Wind Sheltering

The effect of wind sheltering on the final void is very difficult to predict prior to development of the open cut pit.

Based on observations from a small number of voids, McJannet et al, 2019 proposed a wind function for predicting the effect of sheltering based on the depth of the void and the fetch distances. Unfortunately, as the factors in this function are unpublished, the relationship cannot be applied here.

At Mount Goldsworthy void, which has fetch lengths of 300m to 900m (similar to the proposed void), McJannet reported reductions in windspeed at the water surface (70m below the ground surface) of approximately 45%. Using McJannet et al's 2012 wind function, a reduction of 45% from an average windspeed of 2m/s would cause a reduction in the evaporation rate of 26%. However, McJannet has also reported significant increases in windspeed in mine voids at Norwich Park Mine. Computational Fluid Dynamics (CFD) studies of air movement over mine pits show the issue is very complex and site-specific – depending on the shape of the void, prevailing wind directions and thermal effects.

For the purpose of the Monte Carlo analysis, WRM sampled the windspeed reduction at a depth of 70m below ground level (527mAHD) from a symmetrical triangular distribution between 0% and 45%. At higher water elevations, the reduction in windspeed will be interpolated between the sampled value and 0% at the surface level (597mAHD).

The resultant sheltering factors (to adjust evaporation rate) are shown in **Figure 26**. The McJannet et al (2012) wind function will then be used to calculate a "sheltering factor" – the ratio of sheltered evaporation to unsheltered evaporation. The resultant sheltering factors (to adjust evaporation rate) are shown in **Figure 27**.

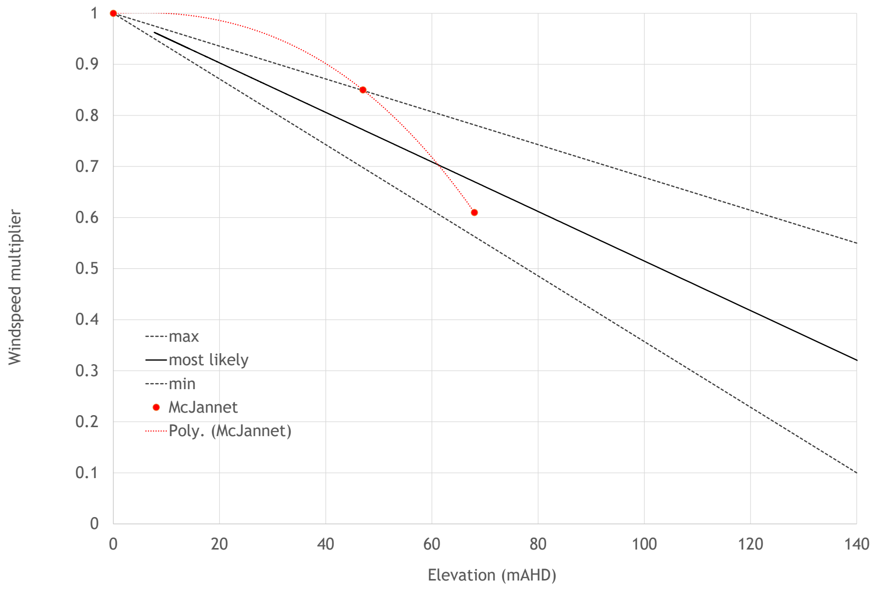

Figure 26
Windspeed multiplier compared to McJannet et al 2016

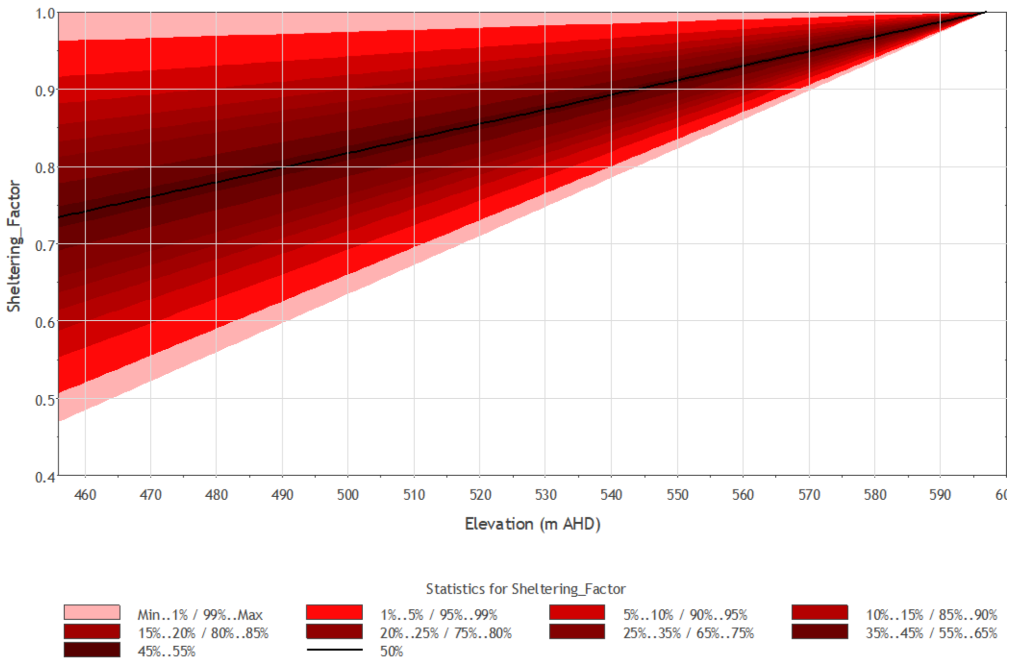

Figure 27
Sheltering factor over full range of elevations